ISSN 2070-2582
Key title: Newsletter (European Association for the Science of Air Pollution. Online)
Abbreviated key title: Newsletter (Eur. Assoc. Sci. Air Pollut., Online)
Parallel title: EURASAP newsletter

Articles, Letters and other Contributions
for the EURASAP Newsletter since 2008
to
Prof. Zvjezdana Bencetić Klaić
Andrija Mohorovičić Geophysical Institute,
Department of Geophysics, Faculty of Science
University of Zagreb
Horvatovac bb, 10000 Zagreb, Croatia
zklaic@gfz.hr

Membership forms
to
Prof. Carlos Borrego
IDAD - Instituto do Ambiente e Desenvolvimento,
Campus Universitário de Santiago,
3810-193 Aveiro, PORTUGAL,
E-mail: rosamfreire@ua.pt

ISSN 2070-2582

EURASAP

Newsletter 72
April 2011

European association for the science of air pollution

EURASAP GOVERNING BODIES

CONTENTS

Front cover: photo by Berislav Rožman

EDITORIAL

Dear EURASAP members,

Three young scientists who obtained EURASAP travel grants, namely, Sabine Banzhaf, Yongfeng Qu and Stavros Solomos, prepared together with their collaborators interesting articles, which you can find in this issue.

Additionally, you will find information on some workshops and conferences dealing with the air pollution that will be held in 2011. The same information is also updated at regular basis at the EURASAP web site http://www.eurasap.org/.

In the News section, you can learn about a non-profit making organisation which aims to disseminate information of atmospheric dispersion modelling - UK Atmospheric Dispersion Modelling Liaison Committee.

At the end, please, check if you have paid the membership fee for 2011.

The Newsletter Editor

Scientists' Contributions -

WET DEPOSITION: MODEL DEVELOPMENT AND EVALUATION

Sabine Banzhaf[1], Peter Builtjes[1,2], Andreas Kerschbaumer[1], Martijn Schaap[2], Eric van der Swaluw[3], Rainer Stern[1] and Eberhard Reimer[1]

[1] Free University Berlin, Institute of Meteorology, Germany
[2] TNO, The Netherlands
[3] National Institute for Public Health and the Environment (RIVM), The Netherlands

Abstract: The Chemistry Transport Model REM-Calgrid (RCG) has been improved by implementing a more detailed description of aqueous-phase chemistry and wet deposition processes including droplet pH. A sensitivity study on cloud and rain droplet pH has been performed to investigate its impact on model sulphate production and gas wet scavenging. Air concentrations and wet deposition fluxes of model runs applying differing droplet pH have been analysed and compared to observations. It was found that droplet pH variation within atmospheric ranges affects modelled air concentrations and wet deposition fluxes significantly.

1. INTRODUCTION

Enhanced deposition fluxes of sulphur and nitrogen compounds damage ecosystems by eutrophying and acidifying soils and fresh water leading to a change of ecosystem diversity (Bobbink et al, 1998; Rabalais, 2002). International co-operations to reduce anthropogenic emissions of acidic precursors have been adopted since the 1980s. However, Critical Loads are still exceeded over large parts of Europe (Lorenz et al, 2008) indicating a continued need for further implementation of air pollution abatement strategies.

Chemistry Transport Models (CTMs) are used to calculate sulphur and nitrogen dry and wet deposition fluxes. The description of wet deposition processes within most CTMs is often rather crude. A multi model evaluation on sulphur and nitrogen wet deposition fluxes (Dentener et al., 2006) including 23 models of different resolution and different complexity in chemistry and physics showed that 60–70% of the calculated wet deposition rates for Europe and North America agreed to within ±50% with measurements. On the regional scale a model inter-comparison over Europe (TNO Report van Loon et al., 2004) showed that modelled wet fluxes usually differ substantially from the observations, they show poor correlation with the observations, and also show a large scatter among the models. Model development concerning the description of cloud chemistry and scavenging processes is needed to improve modelling of wet deposition fluxes and thus the overall model performance.

Sulphur and nitrogen concentrations in the atmosphere impact the pH of atmospheric water droplets. The droplet pH affects the aqueous phase chemistry within the droplet and the mass of scavenged gases by the droplet (Seinfeld and Pandis, 1998). More than two decades ago Scire and Venkatram (1985) found in a model study on the contribution of aqueous-phase SO_2 oxidation to wet scavenging of sulphur components that a significant fraction (30-75%) of sulphate in precipitation is due to pH dependent aqueous-phase oxidation of dissolved SO_2. Recently, Redington et al. (2009) performed a sensitivity study using a Lagrangian dispersion model showing that aqueous-phase sulphate aerosol production is very sensitive to modelled cloud pH. Moreover, accounting for pH dependent cloud chemistry is essential for investigating trends in sulphur concentrations and depositions (Fagerli and Aas, 2008).

However, there are only few studies on the sensitivity of model results to droplet pH. We aim to study the impact of pH-dependent parameterizations on the model performance for wet deposition and concentrations of sulphur and nitrogen components over Germany. In the present study the applied CTM RCG was improved by implementing an enhanced physical and chemical description of scavenging processes and an improved sulphate production scheme including pH dependency. Several model runs were carried out to investigate the sensitivity of sulphate formation and gas wet scavenging to pH variations by analyzing the modeled air concentrations and wet deposition fluxes. Furthermore the model results were compared to observations.

2. METHODS AND DATA

2.1 Chemistry Transport Model

The off-line Eulerian grid model RCG simulates air pollution concentrations solving the advection-diffusion equation on a regular lat-lon-grid with variable resolution over Europe (Stern et al., 2006; Beekmann et al., 2007). RCG was evaluated within many urban and regional applications and within the framework of several European model inter-comparison studies (Hass et al. 1997, Van Loon et al. 2004, Stern et al. 2008, Cuvelier et al. 2006, Vautard et al. 2007, and references therein). For the present study model improvements concerning sulphate production and scavenging processes have been carried out. For the aqueous-phase conversion of dissolved SO_2 to sulphate in cloud water two pathways are considered in the model: oxidation by H_2O_2 and oxidation by dissolved O_3. The upgraded corresponding reaction rates are functions of cloud liquid water content and droplet pH (Seinfeld and Pandis, 1998). The improved RCG wet deposition scheme distinguishes between in-cloud and below-cloud scavenging for gases and particles. The gas in-cloud scavenging coefficient is dependent on the cloud liquid water content and cloud water pH. Moreover, droplet saturation is considered for gas wet scavenging by calculating the maximum possible gas in solution as a function of droplet pH (CAMx, 2010).

2.2 Summary of model runs

All model runs were performed on a domain covering Germany (47.2N-55.1N; 5.4E-15.7E) with a horizontal resolution of approx. $7x7km^2$ and 20 vertical layers up to 5000 m. A large scale RCG run

covering Europe provided the Boundary Conditions. Emissions for Germany were delivered from local and national inventories (Jörß et al., 2010, Thiruchittampalam et al., 2010), while high resolution European emissions are obtained from TNO (Denier van der Gon et al., 2010). Hourly meteorological fields are provided by the analysis system TRAMPER (Reimer und Scherer, 1992). The model sensitivity study was performed over 4 weeks in summer 2005 (05th July- 2nd August 2005). The base run was carried out forcing droplet pH to a constant value of 5 as it is done within the RCG operational version. Sensitivity runs were performed applying a constant droplet pH of 4.5, 5.5, 6 and 6.5 for

Case 1: sulphate production only while gas wet scavenging pH constant at 5;
Case 2: gas wet scavenging only while sulphate production pH constant at 5;
Case 3: sulphate production and gas wet scavenging.

2.3 Observational Data

For evaluation of TRAMPER precipitation, RCG wet deposition fluxes and RCG air concentrations UBA (Umweltbundesamt (=Federal Environment Agency, Germany)) station measurements (UBA, 2004) over Germany were applied. At UBA sites precipitation sampling is performed by using wet-only collectors (Firma Eigenbrodt, Germany) to avoid contributions of dry deposited material. An additional meteorological rain gauge (Joss Tognini or Hellmann) is used for the observations of precipitation amounts. Air concentrations of sulphate are sampled using the filter pack method (EMEP, 1996). Wet deposition fluxes are available as weekly sums while air concentrations are available as daily means.

3. RESULTS AND DISCUSSION

3.1 Model cloud chemistry and gas wet scavenging sensitivity to droplet pH

Figure 1a demonstrates the sensitivity of model sulphate formation to droplet pH (=Case 1). The figure shows the vertical distribution of the domain average sulphate air concentration of the different droplet pH runs for the investigation period. Sulphate concentrations increase with increasing model droplet pH due to a higher sulphate production rate via the O_3 oxidation pathway. Applying a droplet pH of 6.5, average sulphate concentrations increase by up to 46% compared to the base run. The enhancement is most significant for model runs with droplet pH greater 5. For pH lower 5 the reaction rates of oxidation via H_2O_2 are several magnitudes higher than those of the O_3 oxidation pathway. While oxidation by dissolved O_3 varies over wide ranges for atmospheric pH ranges, oxidation by H_2O_2 shows a negligible pH dependency (Seinfeld and Pandis, 1998). However, figure 1a illustrates that using a constant droplet pH of 5 as applied within RCG operational version represents low droplet pH cases adequately while cases with pH values greater 5 are not well represented. Since sulphate production is a SO_2 sink the domain average SO_2 (not shown here) concentration decreases with increasing pH. Figure 1b displays the sensitivity of model gas wet scavenging to droplet pH (=Case 2). The deviation of the domain wet deposition sum from the base run is presented for different droplet pH runs.

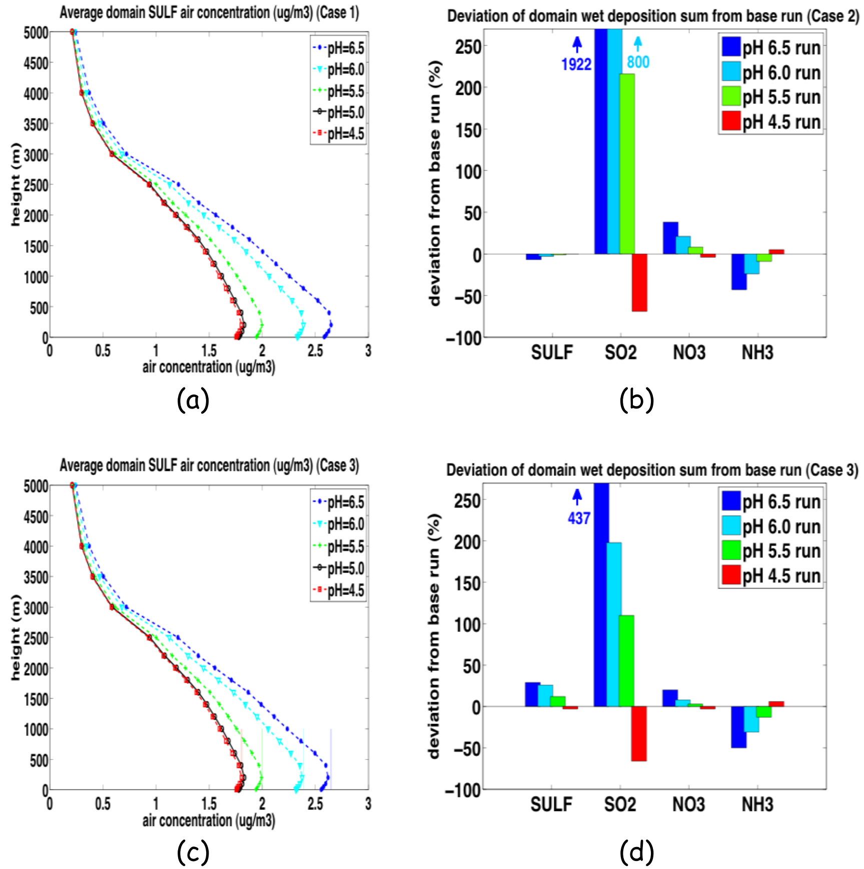

Figure 1. Domain average sulphate air concentration for Case 1 (a) and Case 3 (c) and deviation of the domain wet deposition sum from the base run for Case 2 (b) and Case 3 (d) of the different droplet pH runs for the investigation period

Most significant is the increase of SO_2 wet deposition fluxes with increasing model droplet pH (enhancement by a factor of approx. 20 for the pH 6.5 run). This is because more SO_2 can be dissolved in the droplets as the pH of the latter increases. Similarly, NH_3 wet deposition fluxes decrease with increasing model droplet pH. The decrease is less significant than for SO_2 due to the high solubility of NH_3. The decline of NH_3 wet depositions fluxes leads to higher NH_3 air concentrations resulting in an enhanced formation of ammonium nitrate, and hence to an increase of NO_3 wet deposition fluxes.

Figure 1 (c,d) shows the results of the Case 3 run in which droplet pH was varied within both, sulphate production and gas wet scavenging. Comparing results of Case 3 to results of Case 1 and 2 displays the coupling between sulphate formation and gas wet scavenging processes. In Case 3 the increase of domain average sulphate concentration with increasing pH is slightly damped due to less SO_2 availability with increasing droplet pH caused by higher SO_2 gas wet scavenging rate. Applying a droplet pH of 6.5 average sulphate concentrations now increase by up to 43% compared to the base run instead of by 46% as in Case 1. The increase of domain SO_2 wet deposition sum with increasing pH is with 437% much less than in Case 2. Hence, the more effective sulphate formation in between precipitation events and prior to rain out in clouds dominates the impact of variable pH. Consequently, also sulphate wet deposition increases with increasing pH. Finally, due to higher rate of ammonium sulphate formation with increasing pH in Case 3 less NH_3 is available for ammonium nitrate formation and hence, the increase of NO_3 wet deposition fluxes is lower for Case 3 than for Case 2.

3.2 Model sensitivity to pH and comparison to observations

In Figure 2 results of the investigation on the overall model sensitivity on droplet pH are shown (= Case 3) and compared to observations. Figure 2 (a,b) presents sulphate and ammonia air concentrations of the different model runs of Case 3 compared to observations at the UBA stations Melpitz and respectively Waldhof.

The impact of model droplet pH variation on sulphate and ammonia concentrations is significant. RCG reproduces well the temporal devolution of the observed concentrations for both species and the absolute values are within the right range for all droplet-pH runs. Since pH of atmospheric droplets varies during the investigation period there is not one particular droplet pH run that compares best to the observations over the whole period. Weekly measured rainwater pH ranged from 4.7 to 5.8 at Melpitz and from 4.9 to 5.7 at Waldhof within the investigation period. Periods during which all runs show similar results for sulphate and ammonia concentrations are periods with minor cloudiness and precipitation amounts.

Figure 2 (c,d) shows the modelled SOx and NHx wet deposition fluxes of the model sensitivity runs for the investigation period compared to observations at 17 UBA stations spread over Germany. The analysis of the modelled fluxes demonstrates their significant dependency on droplet pH variation. The comparison of TRAMPER precipitation (not shown here) to precipitation measurements at the 17 UBA stations for July 2005 showed satisfying results exhibiting a correlation of 0.8. However, RCG underestimates SOx wet deposition fluxes for all droplet pH runs. An overestimation of SO_2 and sulphate dry deposition fluxes might be the reason for the underestimation of SOx wet deposition fluxes. The lack of dry deposition flux measurements complicates the assessment of the latter. The budget of sulphur compounds within RCG will be subject of subsequent investigations. The results for NHx wet deposition fluxes on the other hand are encouraging. NHx wet deposition fluxes are simulated within the right range by RCG. The variation of wet deposition fluxes for the different droplet pH runs is considerable and again none of the sensitivity runs represents the observed values best over the whole investigation period since atmospheric droplet pH varied during the analysed period. In a further step the atmospheric droplet pH will be modelled to be able to capture the corresponding variation within the modelled air concentrations and wet deposition fluxes.

4. CONCLUSIONS AND OUTLOOK

The present investigation demonstrates that cloud and rain droplet pH variances within model cloud chemistry and gas wet scavenging schemes have a significant impact on resultant air concentrations and wet deposition fluxes. Applying a droplet pH of 6.5 within the aqueous-phase chemistry and the gas wet scavenging scheme, modelled domain monthly mean sulphate air concentrations increased by up to 43% compared to base run (pH=5). Within the same pH 6.5 run SO_2 wet deposition fluxes increased by even 437% compared to the base run. Comparing modelled sulphate and ammonia air concentrations to observations at two UBA stations has shown that RCG reproduced well the temporal devolution of the observed concentrations for both species and the absolute values were within the right range for all droplet pH runs. SOx wet deposition fluxes

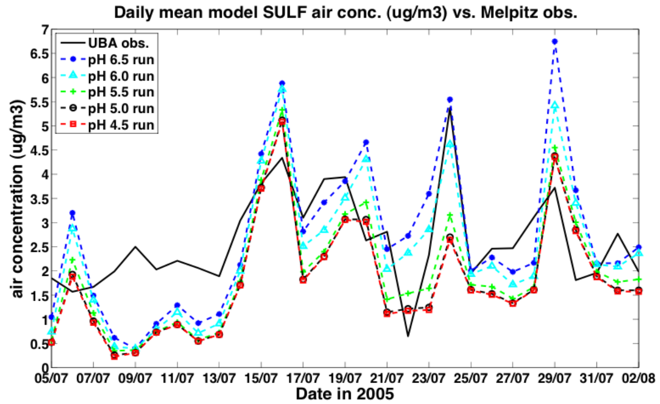

(a)

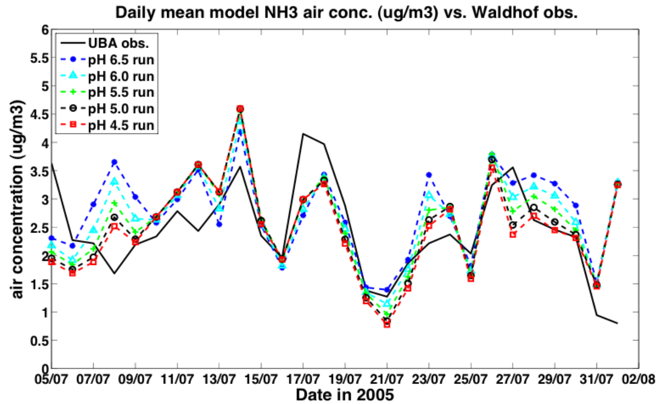

(b)

Figure 2. Modeled and observed sulphate (a) and ammonia (b) air concentrations at UBA station Melpitz respectively Waldhof and modelled and observed SOx (c) and NHx (d) wet deposition fluxes at 17 UBA stations spread over Germany

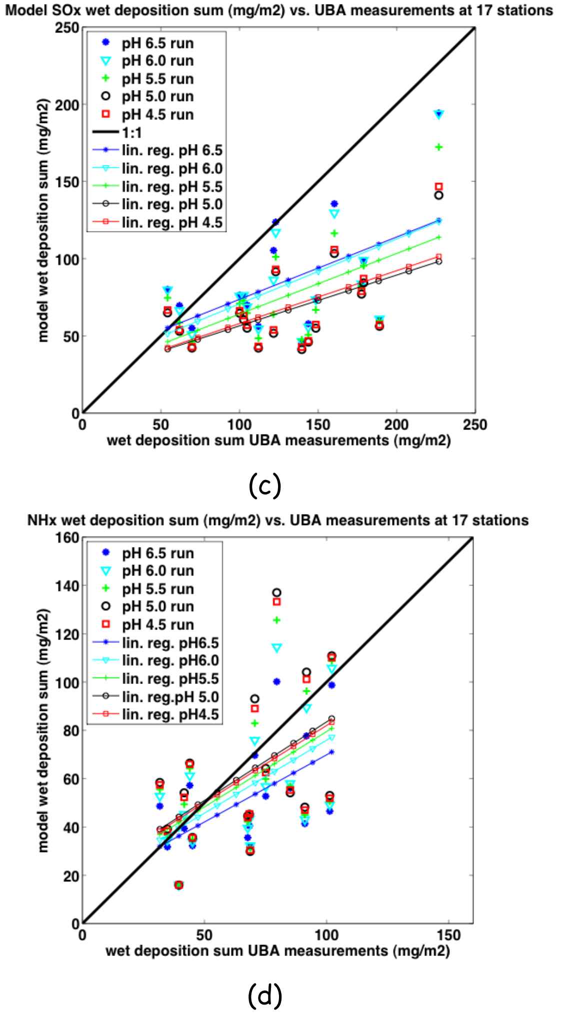

Figure 2. Continuation

were underestimated by RCG while results for NHx were satisfying and indicated a good model performance.

As a next step RCG will be run applying a variable pH of cloud and rain water droplets calculated by using the dissolved species concentrations. First test runs have shown encouraging results indicating an improvement of RCG model skill concerning air concentrations and wet deposition fluxes when applying a modelled droplet pH instead of a constant droplet pH of 5.

REFERENCES

Beekmann, M., Kerschbaumer A., Reimer E., Stern R., Möller D., 2007: PM measurement campaign HOVERT in the Greater Berlin area: model evaluation with chemically specified particulate matter observations for a 1 year period. Atmospheric Chemistry and Physics, 7, 55-68.

Bobbink, R., M. Hornung, and J. M. Roelofs, 1998: The effects of airborne pollutants on species diversity in natural and semi-natural European vegetation, J. Ecol., 86, 717– 738.

CAMx, 2010: User's Guide, Comprehensive air quality model with extensions, Version 5.20, ENVIRON International Corporation, 279 pp.

Cuvelier, C., P. Thunis, R. Vautard, M. Amann, B. Bessagnet, M. Bedogni, R. Berkowicz, J. Brandt, F. Brocheton, P. Builtjes, A. Coppalle, B. Denby, G. Douros, A. Graf, O. Hellmuth, C. Honoré, A. Hodzic, J. Jonson, A. Kerschbaumer, F. de Leeuw, E. Minguzzi, N. Moussiopoulos, C. Pertot, G. Pirovano, L. Rouil, M. Schaap, R. Stern, L. Tarrason, E. Vignati, M. Volta, L. White, P. Wind, A. Zuber, 2006: CityDelta: A model intercomparison study to explore the impact of emission reductions in European cities in 2010. Atmospheric Environment 41 (2007) 189-207.

Denier van der Gon, H., Vischedijk, A., van der Brugh, H., Droge, R., 2010: A high resolution European emission data base for the year 2005, PAREST Paper, Juni 2010.

Dentener, F. , J. Drevet, J. F. Lamarque, I. Bey, B. Eickhout, A. M. Fiore, D. Hauglustaine, L. W. Horowitz, M. Krol, U. C. Kulshrestha, M. Lawrence, C. Galy-Lacaux, S. Rast, D. Shindell, D. Stevenson, T. Van Noije, C. Atherton, N. Bell, D. Bergman, T. Butler, J. Cofala,B. Collins, R. Doherty, K. Ellingsen, J. Galloway, M. Gauss, V. Montanaro, J. F. Müller, G. Pitari, J. Rodr guez, M. Sanderson, F. Solmon, S. Strahan, M. Schultz, K. Sudo, S. Szopa, and O. Wild, 2006: Nitrogen and sulfur deposition on regional and global scales: A multimodel evaluation. Global Biogeochem. Cycles, 20, GB4003.

EMEP Co-operative Programme for Monitoring and Evaluation of the Long-range Transmission of Air Pollutants in Europe, 1996: EMEP manual for sampling and chemical analysis. EMEP/CCC-Report 1/95. Norwegian Institute for Air Research.

Fagerli, H. and W. Aas, 2008: Trends of nitrogen in air and precipitation: Model results and observations at EMEP sites in Europe, 1980–2003. Environmental Pollution. 154, 3, 448-461. doi:10.1016/j.envpol.2008.01.024

Hass, H., P. Builtjes, D. Simpson and R. Stern, 1997: Comparison of model results obtained with several European regional air quality models, Atmos. Environ. 31 (1997) 3259-3279.

Klotz, V., J. Theloke, B. Thiruchittampalam, U. Kugler, T. Geftler, M. Uzbasich, R. Köble, R. Friedrich, U. Dämmgen, R. Stern, P. Builtjes, H. Denier van der Gon, A. Kuhn, 2009: An integrated measure-based approach to fulfil European air quality targets cost-effective on a national level - First results of the German PAREST-project. TFIAM Meeting, 10. Juni, Bilthoven, Netherlands.

Lorenz M., Nagel, H.-D. , Granke O., Kraft P., 2008: Critical loads and their exceedances at intensive forest monitoring sites in Europe. Environmental Pollution 155: 426-435.

Rabalais, N. N., 2002: Nitrogen in aquatic ecosystems, Ambio, 31(2), 102–112.

Redington A.L., R.G. Derwent , C.S. Witham , A.J. Manning, 2009: Sensitivity of modeled sulphate and nitrate aerosol to cloud, pH and ammonia emissions. Atmospheric Environment, Volume 43, Issue 20, pp. 3227–3234.

Reimer, E. and Scherer, B., 1992: An operational meteorological diagnostic system for regional air pollution analysis and long-term modeling. Air Pollution Modelling and its Application IX, Kluwer Academic/Plenum Publisher, New York.

Scire, J.S. and A. Venkatram, 1985: The contribution of in-cloud oxidation of SO_2 to wet scavenging of sulfur in convective clouds. Atmospheric Environment, Volume 19, Issue 4, pp. 637-650.

Seinfeld, J.H. and N. Pandis, 1998: Atmospheric Chemistry and Physics: From Air Pollution to Climate Change. John Wiley and Sons, Inc., New York, 1326 pp.

Stern, R., Yamartino, R., Graff, A., 2006. Analyzing the response of a chemical transport model to emissions reductions utilizing various grid resolutions. In: Twenty-eighth ITM on Air Pollution and its Application., May 15-19, 2006, Leipzig, Germany.

Stern R., P. Builtjes, M. Schaap, R. Timmermans, R. Vautard, A. Hodzic, M. Memmesheimer, H. Feldmann, E. Renner, R. Wolke, A. Kerschbaumer, 2008: A model inter-comparison study focussing on episodes with elevated PM10 concentrations. Atmos. Env., 42, 4567-4588.

Thiruchittampalam, B., Köble, R., Theloke, J., Kugler, U., Uzbasich, M., Geftler, T.: „Dokumentation des PAREST Emissionsverteilungsmodells für Deutschland“ PAREST-Bericht Juli 2010.

UBA, 2004: Manual for Quality Assurance (in German), Texte 28/04, ISSN 0722-186X, Umweltbundesamt – Berlin, Fachgebiet II 5.6, 536 pp.

Van Loon M., Roemer M.G.M., Builtjes P.J.H., 2004: Model intercomparison in the framework of the review of the Unified EMEP model, TNO report R2004/282.

Vautard R., P. Builtjes, P. Thunis, K. Cuvelier, M. Bedogni, B. Bessagnet, C. Honoré, N. Moussiopoulos, M. Schaap, R. Stern, L. Tarrason and M. van Loon, 2007: Evaluation and intercomparison of Ozone and PM10 simulations by several chemistry-transport models over 4 European cities within the City-Delta project, Atmospheric Environment 41 (2007), pp. 173–188.

MODELING OF THE URBAN ENERGY BALANCE TAKING INTO ACCOUNT FLUID MECHANICS WITH METEOROLOGICAL IN AN IDEALIZED URBAN AREA

Yongfeng Qu[1], Maya Milliez, Luc Musson Genon, Bertrand Carissimo

CEREA, Teaching and Research Centre in Atmospheric Environment, Joint laboratory ENPC/EDF R&D, 6-8 avenue Blaise Pascal, 77455 Marne la Vallée, France

[1]yongfeng.qu@cerea.enpc.fr

Abstract: In order to take into account atmospheric radiation and the thermal effects of the buildings in simulations of atmospheric flow and pollution dispersion in urban areas, we have developed a three-dimensional atmospheric radiative scheme in the atmospheric module of the open-source CFD model Code_Saturne. This paper describes our ongoing work on the development of this model. The radiative scheme has been previously validated with idealized cases and the results of a real case. Here we present results of the full coupling of the radiative and thermal schemes with the 3D dynamical flow model. First, we show the influence of airflow on surface temperature. Secondly, we discuss the impact on airflow of radiative transfers.

Keywords: urban energy model, 3D atmospheric radiation, CFD

INTRODUCTION

Urban and rural environments differ substantially in their micro-climate. In a city, concrete, asphalt, and glass replace natural vegetation, and vertical surfaces of buildings are added to the normally flat natural rural landscape. Urban surfaces generally have a lower albedo, greater heat conduction, and more heat storage than the surfaces they replaced. The geometry of city buildings causes the absorption of a greater quantity of available incoming solar radiation and outgoing terrestrial infrared radiation. Even in early morning and late afternoon the urban areas are intercepting and absorbing radiation on their vertical surfaces. In urban areas, large amounts of heat energy are added to the local energy balance through transportation, industrial activity, and the heating of buildings. Urban areas tend to be warmer than the surrounding countryside. These differences in temperature are best observed at night under stable conditions when atmospheric mixing is at a minimum. Climatologists call this phenomenon the urban heat island. The urban heat island is strongest at the city centre where population densities are highest and industrial activity is at a maximum. The heat island effect has been described in many cities around the world, and temperature differences between city and country can be as high as 6° C.

Wind in urban areas is generally calmer than those in rural areas. This reduction in velocity is due the frictional effects of the city's buildings. However, some street and building configurations within a city can locally channel the wind and increase its velocity through a venturi effect.

For understanding the unique features of urban climates, there have been many studies in real cities in which data was

acquired using towers, aircraft, and satellites (Masson et al., 2008). Also, by working with a uniform built-up area, the results are easier to interpret and more suitable for urban modelling than data from real cities (Yee and Biltoft, 2003; Kanda et al., 2005).

Since interest in urban climatology has increased in the past decade, a topic of interest corresponds to the thermal and dynamical airflow response to the urban system solicitations, resulting in radiative transfers and convective exchanges within the urban air and with the building walls (Grimmond and Oke, 1999; Arnfield, 2003).

In the past few years, numerical studies have been conducted using two dimensional urban model (e.g. the Town Energy Balance (TEB) scheme (Masson 2000)) to describe the fundamental impact of the urban models. Two-dimensional canyon models allow for the explicit representation of the two horizontal components and the vertical component of idealized urban surfaces: roofs, roads and walls, respectively. In addition, multiple reflection and radiative interaction effects, wind sheltering, and explicit urban canopy layer air temperatures and energy balances may be incorporated within this framework. Many three-dimensional models have been developed in the recent years to simulate dynamics and thermodynamics of the urban atmosphere with various degree of simplification (Miguet and Groleau 2002; Gastellu-Etchegorry et al. 2004; Kanda et al. 2005; Krayenhoff and Voogt 2007; Asawa et al. 2008). These models aim to solve the Surface Energy Balance (SEB) for a 3D urban canopy. They share in common the following parameterizations in their design: the schemes possess separate energy budgets for roofs, roads, walls; radiative interactions between roads and walls are explicitly treated, but all rely on simplified convective transfer.

In order to more accurately model the airflow in the urban canopy in non neutral conditions and take into account the three dimensional convective exchanges, we developed a three-dimensional microscale radiative model coupled with a 3D CFD code for complex geometries to simulate dynamics and thermodynamics of the urban atmosphere (Milliez et al. 2006). Differing from other radiative models which calculate the view factors (UCLCM, TUF-3D, DART, SOLENE and 3D-CAD) to estimate the incoming radiative fluxes on urban surfaces, our model directly solves the 3D radiative transfers equation in the whole fluid domain. This approach might be less precise in the calculation of the radiosity, but allow us to determine the radiation flux not only on the facets of the urban landscape but also in each fluid grid cell between the buildings. The purpose of the present work is to study the full radiative-dynamical coupling, using an evolving 3D flow field. First, we present the model and then discuss in detail the results of the full coupling. We further discuss the thermal impact of buildings on airflow in an idealized urban area.

EQUATIONS AND MODEL DESIGN

As a key parameter, surface temperature (T_w) is determined by the surface energy balance and is related in a fundamental way to each of its component fluxes (Fig. 1). S^*, the net short-wave radiative flux which is the difference between incoming and outgoing short-wave radiation. L^*, the net long-wave radiative flux which is the difference between outgoing long-wave radiation from the surface and incident atmospheric long-wave radiation. The sensible heat flux term convected from the surface is noted the Q_H. Another important factor is the conductive exchanges (Q_{cond}) within the

building which link the surface temperature to the internal building temperature.

a. CFD model

The simulations are performed with the 3D open-source CFD code *Code_Saturne* which can handle complex geometry and complex physics. In this work, we use the atmospheric module, which takes into account the larger scale meteorological conditions and the stratification of the atmosphere. In our simulations, we use a Reynolds Averaged Navier-Stokes (RANS) approach with a k-ε turbulence closure. The numerical solver is based on a finite-volume approach for co-located variables on an unstructured grid. Time discretization is achieved through a fractional step scheme, with a prediction-correction step (Archambeau et al., 2003; Milliez and Carissimo, 2007, 2008).

The thermal energy equation of the flow is solved, both to determine stratification effects on vertical turbulent transport and to estimate the surface-air thermal gradient that controls convective heat transfer. Our model solves the 3D RANS equations in the entire fluid domain. We use a rough wall boundary condition in our simulations. The heat transfer coefficient is computed for each solid sub-facet, depending on the local friction velocity and the thermal stratification:

$$h_f = \frac{\rho C_p u_* \kappa f_m}{\sigma_t \ln(\frac{d+z_0}{z_{0T}})\sqrt{f_h}} \qquad (1)$$

where ρ is flow density, C_p specific heat, u_* is the friction velocity which is determined by iteration, k is von Karman constant, σ_t turbulent Prandtl number, d is distance to the wall, z_0 the roughness length, z_{0T} the thermal roughness length, f_m and f_h are the Louis explicit stability functions (Louis, 1979).

b. Radiative model

We chose the Discrete Ordinate Method (Fiveland 1984; Truelove 1987; Liu et al. 2000) to resolve the radiative transfer equation. The resolution of the numerical method is based on the radiative wave directionally propagating. The spatial discretization used the same mesh as in the CFD model. The angular discretization has two options, 32 or 128 directions.

b.1. Short and long-wave radiation

As usually done, we separate the atmospheric radiation into short-wave and long-wave radiation. The total incoming and outgoing short-wave radiative fluxes for each solid surface are given by:

$$S^{\downarrow} = S_D + S_f + S_e \qquad (2)$$

$$S^{\uparrow} = a S^{\downarrow} \qquad (3)$$

where $S^{\downarrow}$ and $S^{\uparrow}$ are respectively the incoming and outgoing short-wave radiative fluxes (W m^{-2}), S_D the direct solar flux (W m^{-2}), S_f the solar flux diffused by the upper atmosphere (W m^{-2}), S_e the flux resulting from the multi-reflections on the other sub-facets (W m^{-2}) and a the albedo of the surface.

We express the long-wave radiation flux for each surface as:

$$L^{\downarrow} = L_a + L_e \qquad (4)$$

$$L^{\uparrow} = \varepsilon \sigma T_{sfc}^4 + (1-\varepsilon)(L_a + L_e) \qquad (5)$$

where $L^{\downarrow}$ and $L^{\uparrow}$ are respectively incoming and outgoing long-wave radiation flux (W m^{-2}), ε the emissivity of the surface, σ the Stefan-Boltzmann constant (5.66703×10^{-8} W $m^{-2}K^{-4}$), T_{sfc} the surface temperature (K), L_a and L_e are the long-wave radiation flux from the atmosphere and from the multi-reflection on the other surface. At the scale of our simulations, we can assume that the atmosphere between the buildings is transparent and set the absorption coefficient to zero.

b.2. Surface temperature model

The surface temperature is obtained with the force-restore approach (Deardorf 1978). The force-restore approach is commonly used in order to calculate the surface temperature in meteorological models. This approach is considered as a very useful tool where a prognostic equation for temperature is used in order to reproduce exactly the response to periodic heating of the soil. It is true that it may not be the best suited for our experiments, for which the buildings are made by shipper containers. However, since it is a simple model, we adapted it to the surface of the buildings as a preliminary approach (Johnson et al. 1991):

$$\frac{\partial T_{sfc}}{\partial t} = \frac{\sqrt{2\omega}}{\mu} Q^* - \omega (T_{sfc} - T_{g/b}) \qquad (6)$$

where T_{sfc} is the surface temperature (K), ω the earth angular frequency (Hz), μ the thermal admittance (J m^{-2} $s^{-0.5}$ K^{-1}) and $T_{g/b}$ either deep soil or internal building temperature (K). Q^* is the total net flux (W m^{-2}) at the wall, which can be expressed as:

$$Q^* = L^* + S^* - Q_H - Q_{LE} - Q_F \qquad (7)$$

with L^* and S^* being net long and short-wave flux (W m^{-2}), respectively, Q_H the sensible heat flux (W m^{-2}), Q_{LE} the latent heat flux (W m^{-2}), Q_F the anthropogenic heat flux (W m^{-2}). Since the site chosen in this study is in the desert, we expect the Q_{LE} and Q_F to be small and neglect them.

In a real building with a good insulation, the variation of the internal building temperature is small which may have little influence on the surface temperature. Taking a constant internal building temperature is well adapted to the force-restore model because the change of the temperature in the deep soil in the diurnal cycle is almost neglected. However the experiments which we simulated here used an unusual building, shipping container. The internal temperature shows its importance which influences much the surface temperature, but was not measured in our experiments. Therefore we applied an internal building temperature evolution equation (Masson et al. 2002):

$$T^{n+1} = T^{n-1}\left(\frac{\tau - \Delta t}{\tau}\right) + \underline{T}\left(\frac{\Delta t}{\tau}\right) \qquad (8)$$

where T^{n+1} and T^{n-1} are the temperatures at the future and previous time step, respectively, Δt is the time step, τ is equal to 1 day, and $\underline{T}$ is the average of the surface temperatures.

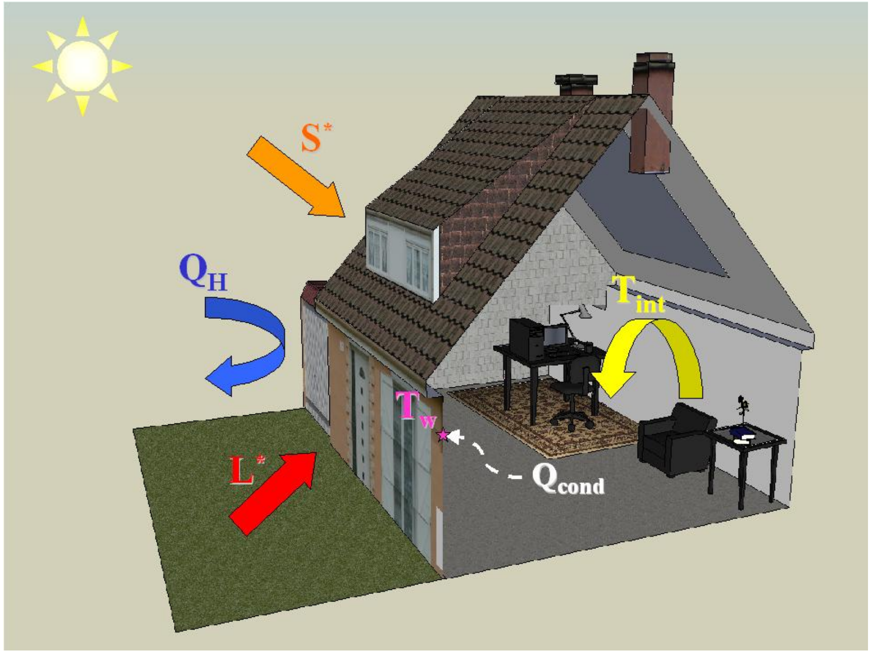

Figure 1. Schematic representation of the energy exchanges at an urban surface (S*: Net short-wave radiative flux; L*: Net long-wave radiative flux; Q_H: Sensible heat flux; Q_{cond} : Conduction heat flux; T_W: Wall surface temperature; T_{int} : Internal building temperature).

RESULTS-DISCUSSION

a. Description of the study configuration

The configuration studied was an idealized urban canopy and its micro-climatic environment, Mock Urban Setting Test (Yee and Biltoft 2004). It was conducted in the Utah desert using 120 shipping containers (L×W ×H: 12.2×2.42×2.54 m) arranged in a regular array. MUST has already been used to validate the dynamics and dispersion model (Hanna et al. 2002; Milliez and Carissimo 2007, 2008). Since temperature data are also provided, we used the MUST field experiment to study in detail the dynamic-radiative coupling. We focused our study on one instrumented container within the array and therefore the domain was reduced to three rows of three containers with an optimum domain size (Fig.2).

b. Description of the meteorological conditions

From the MUST experiment (Biltoft 2001), we chose to simulate the day of September 25th 2001. It is the day which we had a complete 24-hours data set for the upstream wind and the surface temperature which was not the case for other days. During this day, the wind velocity varied from U_{min} = 3 m s^{-1} to U_{max} = 11.5 m s^{-1}, the average air temperature is about 24 °C (measured at 10 m). It is a strong wind case (U_{mean} =7 m s^{-1}) which we have already simulated for studies on dispersion (Milliez and Carissimo 2007). For our coupling study, the wind speed may be too high to test the radiative effects on the airflow, but it emphasizes the convective effects on the surface temperature.

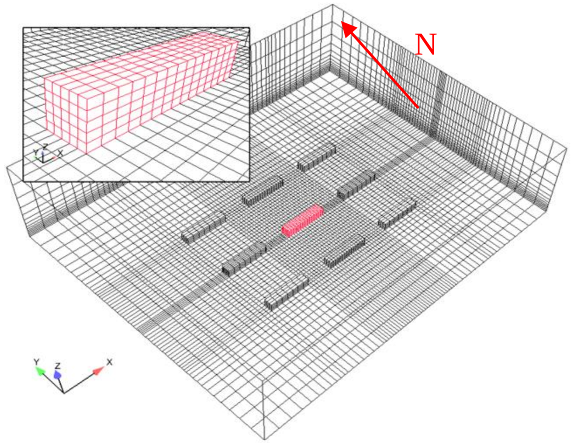

Figure 2. Mesh of the domain and zoom on the sub-domain with the 0.8×0.5×0.5 m resolution.

c. Validation: the influence of airflow on surface temperature

A sensitivity study showed that our radiative and surface temperature models are very sensitive to surface parameters. The boundary conditions are an essential feature of any CFD simulation. In order to be consistent with the experiment, the wind inlet boundary conditions are determined from measurements, using a meteorological file which gives, every 2 hours, the wind velocity, turbulence kinetic energy, dissipation rate and temperature profiles. The variation of the deep soil temperature is neglected. The internal building temperature is computed by the evolution equation with T from measurements. We take same value of the roughness length z_0 as Eichhorn and Balczo (2008). The thermal roughness length z_{0T} is simply considered as 1/10 of z_0. Since the thermal properties of containers are not available in the data, we took the values of albedo, emissivity and the thermal admittance from the literature (Oke

1987; Johnson et al. 1991) for the corrugated iron. Except for the soil albedo: it was evaluated from the incoming and outgoing solar fluxes measured upstream by pyramometers, depending on the zenithal angle.

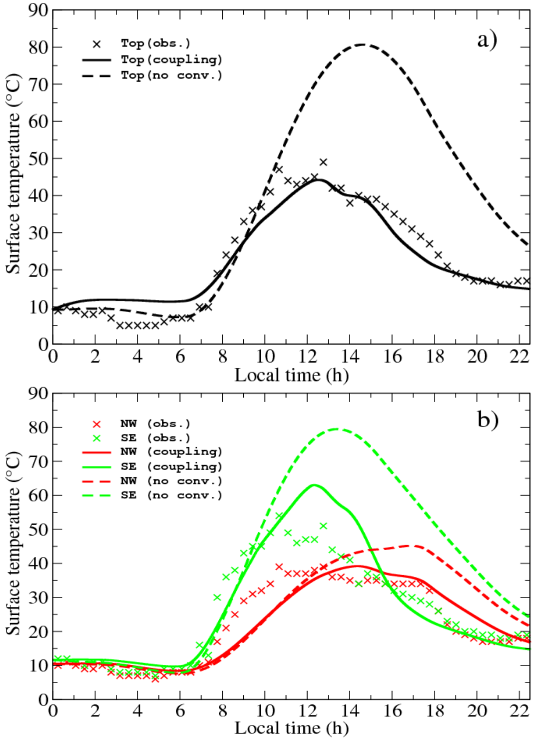

Figure 3. Evolution of surface temperature of roof (top), N-W, S-E, N-E and S-W faces modeled using the force-restore method during a diurnal cycle (X: Measurements; Dashed line: Simulation with radiation only; Straight line: Simulation with the dynamic-radiative coupling).

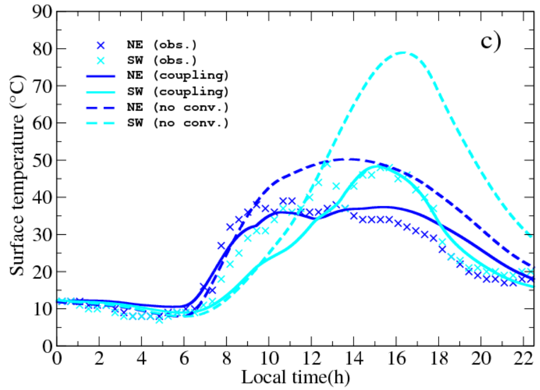

Figure 3. Continuation

Figure 3 shows the evolution of modeled and measured surface temperatures using the force-restore method, with two modeling approaches: only-radiative model (meaning with the convective flux set to zero) and coupled radiative and dynamical model. The diurnal evolutions of the surface temperatures of the top face, S-E face, N-E face are correctly reproduced by the coupled model. The N-W face and S-W face, temperatures show a delay in warming. This may be due to the conduction between the walls that is not taken into account in the simulations. The force-restore model is able to simulate temperatures of urban surfaces which have a good insulation rather than the special surfaces used in MUST experiment. However, in the afternoon the modeled surface temperatures compare well with the measurements. The simulation results show a large difference between the coupled model and only-radiative model, showing the importance of accurately including the effect of convection in microscale modelling (Qu et al., 2010).

d. Discussion: the impact on airflow of radiative transfers

The influence of wall heating in street canyons due to solar radiation incident on one or more walls under conditions of low wind speed is another topic of interest. The investigations about the thermal effects on the airflow in a street canyon (Kovar-Panskus et al., 2002) are usually not including a radiative model. As an extension to the MUST study, we simulated the following ideal case: an inlet airflow perpendicular to the streets with a 10 m-wind speed of 1 m/s, from 12h to 12h15. The initial soil and wall temperatures were set to 30°C and 40°C respectively. In order to highlight the thermal effect on the air flow, air temperature is usually initialized to a very low value (5°C in Sini et al., 1996, Kovar-Panskus et al., 2002). According to MUST experience, we set the air temperature to 30°C which is more realistic. In addition, we modified the cavity aspect ration (W/H) to 1 from the MUST site in order to emphasize the thermal impact on the wind.

Figure 4 illustrates the distribution of the mean vertical velocity W on the centre-plane for three thermal situations: no heating, uniform wall heating and realistic wall heating from radiative transfers. The wind patterns under each condition are obviously different. Without heating (neutral case, Fig 4.1), the airflow pattern in the canopy is a classic skimming flow regime. In the wall heating case (Fig 4.2), the air is significantly accelerated upward along the heated wall. It interrupts the flow from the top of the canopy. In the solar-induced wall heating case (Fig 4.3), the distribution of W differs from the uniform wall heating case. Indeed, taking into account the position of the sun and the shading effects, the walls are not heated uniformly, modifying the stratification of the flow and hence the buoyancy forces. Moreover,

the difference between the distribution of the mean temperature under the uniform wall heating and the radiative transfer conditions is complex to discuss. It can be more important depending on which kind of building parameters we use in the radiative scheme, for instance, the property of material. In Figure 5, we illustrate the air temperature under the same radiative transfer conditions by only changing the value of the albedo of the building wall. The three thermal plumes appear similar, but close to the wall we can observe more than 2 Kelvin difference inside of the thermal plumes.

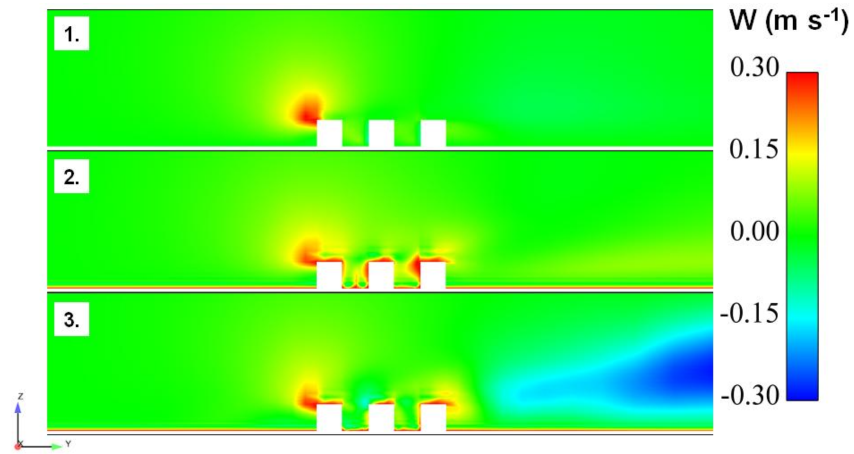

Figure 4. Mean vertical velocity distribution on centre-plane, 1) neutral case; 2) wall heating; 3) radiative transfer.

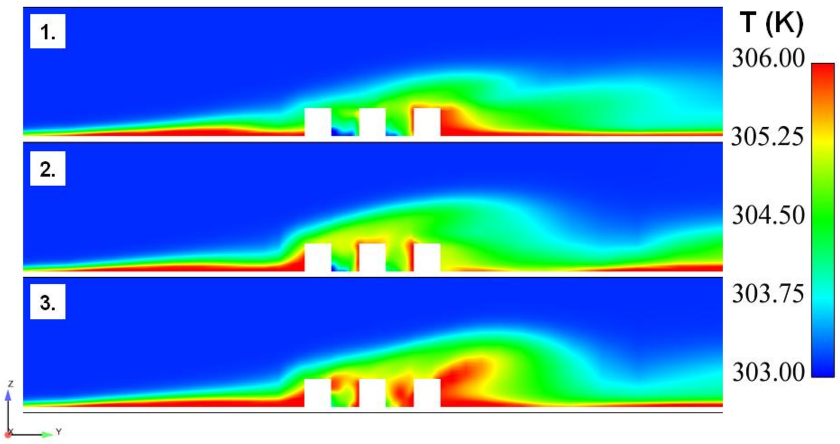

Figure 5. Air temperature under the same radiative transfer conditions by only changing the value of the albedo of the building wall: 1) α=0.1; 2) α=0.3; 3) α=0.8.

In order to analyze qualitatively the thermal impact on the airflow, we plotted several vertical profiles of the different variables at different positions in the domain as shown in Figure 6. As an example, in Figure 6a., b, and c, we compare the vertical profiles of potential temperature, vertical velocity and turbulent kinetic energy respectively on the roof of the building under different thermal conditions. Without the shadow effects, the air temperature is higher on the roof in the solar-induced wall heating case (Fig 6.a). With 0.1 as the value of the albedo of the building wall, the difference of temperature with the uniform wall heating case is already close to 1K in this short simulation. Taking into account the thermal stratification, the vertical component of the velocity shows a large variability in non neutral cases (Fig 6.b). As shown in figure 6.c, the impact of the heating on the turbulent kinetic energy is also very important at these low wind speeds (25% increases in wall heating condition; doubled in radiative transfer conditions with 0.1 as the value of the albedo).

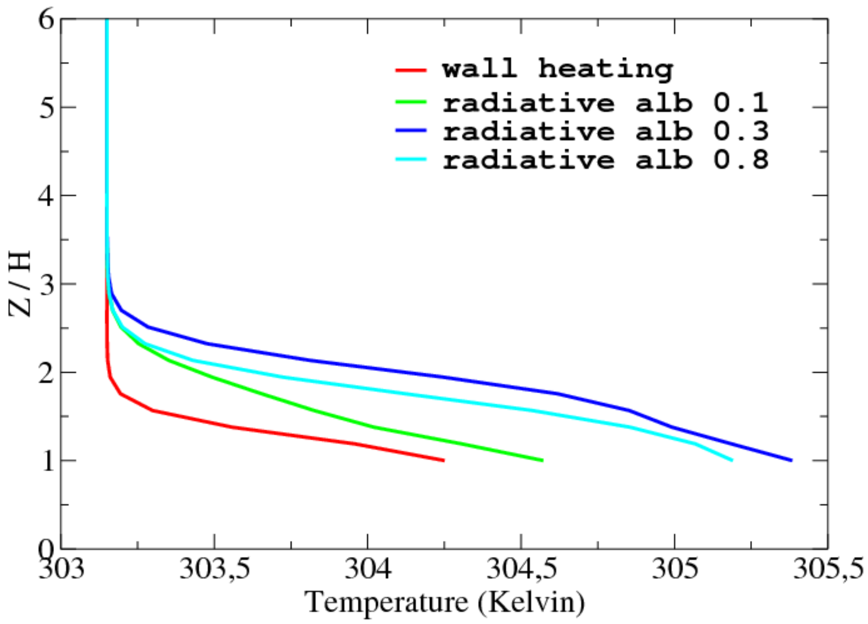

(a)

Figure 6. Vertical profiles of (a) temperature (Kelvin); (b) vertical velocity; (c) turbulent kinetic energy ($m^2\ s^{-2}$) on the roof.

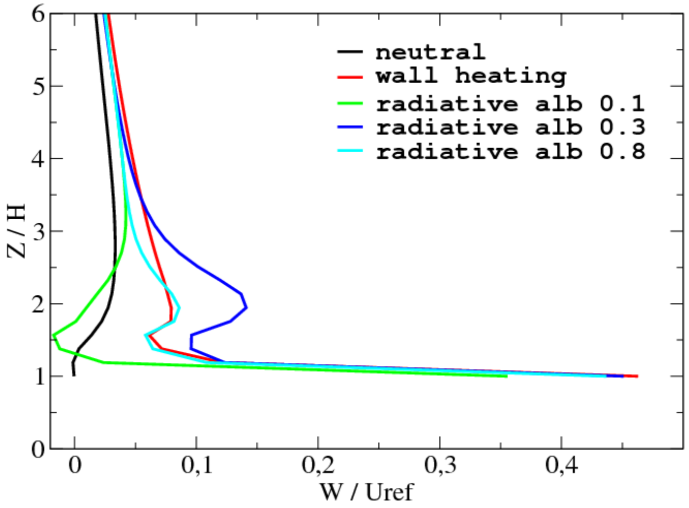

(b)

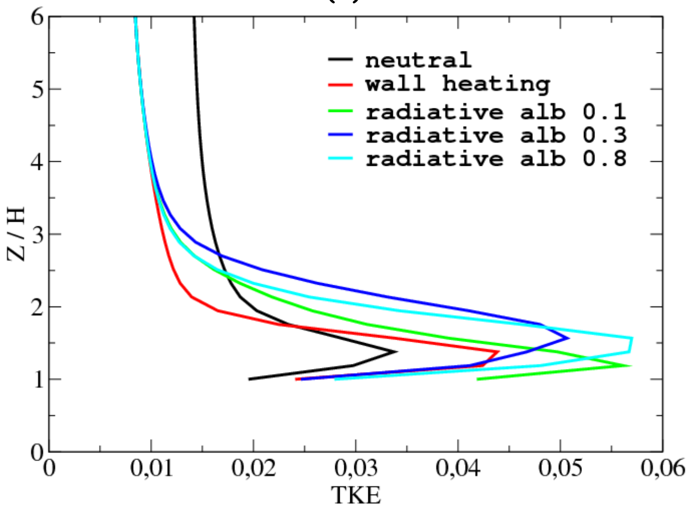

(c)

Figure 6. Continuation

CONCLUSION

New atmospheric radiative and thermal schemes were implemented in the atmospheric module of a three-dimensional CFD code (*Code_Saturne*). The model was evaluated with the field measurements from an idealized urban area, the MUST field experiment. The improved model is able to reproduce the evolution of the surface temperatures for different faces of a container during a diurnal cycle. The impact of convective effect on the surface temperature is significant. Since the force-restore method may be more suited for insulated buildings with a really constant internal temperature, may not be well adapted to the MUST containers. Nevertheless, using an appropriate evolution equation for the interior buildings, depending on the surface temperatures of the previous radiative time step, the force-restore shows good results during afternoon but less accuracy at sunset. After that we analyze additional idealized simulations. We discussed the effects of different wall heating conditions on the airflow in a low wind speed case. After 15 minutes, the airflow pattern is different. The results show the importance of the stratification effects in urban areas in this case and the contribution of realistic radiative transfers within the canopy. The work can be useful in wind engineering and pollutant dispersion applications. But this discussion is based on an idealized urban area. At microscale, small irregularities can break the periodic flow patterns found in a regular array of containers with identical shapes. That is the reason why we will evaluate the coupled dynamic-radiative model on a district of a real urban area with the CAPITOUL field experiment (City of Toulouse, France).

REFERENCES

Archambeau, F., N. Méchitoua, and M. Sakiz, 2003: Code Saturne : a Finite Volume Code for the Computation of Turbulent Incompressible Flows - Industrial Applications. Int J Finite Volumes, 1, 1–62.

Arnfield, A. J., 2003: Two decades of urban climate research: A review of turbulence, exchanges of energy and water, and the urban heat island. Int. J. Climatol., 23 (1), 1–26.

Asawa, T., A. Hoyano, and K. Nakaohkubo, 2008: Thermal design tool for outdoor space based on a numerical simulation system using 3d-cad. Build.Environ., 43, 2112–2123.

Biltoft, C. A., 2001: Customer report for mock urban setting test. DPG Document WDTC-FR-01-121, West Desert Test Center, U.S. Army Dugway Proving Ground, 58 pp., Dugaway,

Deardorf, J. W., 1978: Efficient prediction of ground surface temperature and moisure with inclusion of a layer of vegetation. J. Geophys. Res., 83, 1889–1903.

Eichhorn, J. and M. Balczo, 2008: Flow and dispersal simulations of the Mock Urban Setting Test. 12th Int. Conf. on Harmonisation within Atmospheric Dispersion Modelling for Regulatory Purposes, Cavtat, Croatia (October 6-9, 2008).

Fiveland, W. A., 1984: Discrete-ordinates solutions of the radiative transport equation for rectangular enclosure. J. Heat Tran., 106, 699–706.

Gastellu-Etchegorry, J., E. Martin, and F. Gascon, 2004: Dart: A 3-d model for simulating satellite images and surface radiation budget. Int J. of Remote Sens., 25, 75–96.

Grimmond, C. S. B. and T. R. Oke, 1999: Heat storage in urban areas: Local-scale observations and evaluation of a simple model. J. Appl. Meteor., 38, 922–940.

Hanna, S. R., S. Tehranian, B. Carissimo, R.W. Macdonald, and R. Lohner, 2002: Comparisons of model simulations with observations of mean flow and turbulence within simple obstacle arrays. Atmospheric Environment, 36, 5067–5079.

Johnson, G. T., T. R. Oke, T. J. Lyons, D. G. Steyn, I. D.Watson, and J. A. Voogt, 1991: Simulation of surface urban heat islands under 'ideal' conditions at night. part i: Theory and tests against field data. Bound.-Layer Meteor., 56, 275–294.

Kanda, M., T. Kawai, M. Kanega, R. Moriwaki, K. Narita, and A. Hagishima, 2005: A simple energy balance model for regular building arrays. Bound.-Layer Meteor., 116, 423–443.

Krayenhoff, E. S. and J. A. Voogt, 2007: A microscale three-dimensional urban energy balance model for studying surface temperatures. Bound.-Layer Meteor., 123, 433–461.

Kovar-Panskus, A., Moulinneuf, L., Savory, E., Abdelqari, A., Sini, J.F., Rosant, J.M., Robins, A., Toy, N., 2002. Water, Air and Soil Pollution: Focus 2: 555-571.

Liu, J., H. M. Shang, and Y. S. Chen, 2000: Development of an unstructured radiation model applicable for two-dimensional planar, axisymmetric, and three-dimensional geometries. J. Heat Tran., 66, 17–33.

Louis, J., 1979: A parametric model of vertical eddy fluxes in the atmosphere. Bound.-Layer Meteor., 17, 187–202.

Masson, V., 2000: A physically based scheme for the urban energy budget in atmospheric models. Bound.-Layer Meteor., 94, 357–397.

Masson, V., C. S. B. Grimmond, and T. R. Oke, 2002: Evaluation of the town energy balance (TEB) scheme with direct measurements from dry districts in two cities. J. Appl. Meteor., 41, 1011–1026.

Masson, V., et al., 2008: The canopy and aerosol particles interactions in toulouse urban layer (CAPITOUL) experiment. Meteor. Atmos. Phys., 102, 135–157.

Miguet, F. and D. Groleau, 2002: A daylight simulation tool for urban and architectural spaces - application to transmitted direct and diffuse light through glazing. Build. Environ., 37, 833–843.

Milliez, M., 2006: Modélisation micro-météorologique en milieu urbain: dispersion des polluants et prise en compte des effets radiatifs. Ph.D. thesis, Ecole des Ponts ParisTech, 228 pp., [Available on line at http://cerea.enpc.fr/fr/theses.html].

Milliez, M. and B. Carissimo, 2007: Numerical simulations of pollutant dispersion in an idealized urban area, for different meteorological conditions. Bound.-Layer Meteor., 122 (2), 321–342.

Milliez, M. and B. Carissimo, 2008: CFD modelling of concentration fluctuations in an idealized urban area, for different meteorological conditions. Bound.-Layer Meteor., 127, 241–259.

Milliez, M., L. Musson-Genon, and B. Carissimo, 2006: Validation of a radiative scheme for CFD modelling of heat transfers between buildings and flow in urban canopies. Preprints, 6th Int. Conf. on Urban Climate, Goteborg, Sweden (June 12-16 2006).

Oke, T. R., 1987: Boundary Layer Climates. 2d ed., Routledge, 435 pp.

Qu, Y., Milliez, M., Musson-Genon, L., Carissimo, B., 2010. 'Development of a building resolving atmospheric CFD code taking into account atmospheric radiation in complex geometries', Preprints of the 31th International Technical Meeting on Air Pollution Modelling and its Application, Torino, Italy; September 26 - October 1.

Sini, J. F., S. Anquetin, and P. Mestayer, 1996: Pollutant Dispersion and Thermal Effects in Urban Street Canyons. Atmospheric Environment, 15, 2659–2677.

Yee, E. and C. A. Biltoft, 2004: Concentration fluctuations measurements in a plume dispersing through a regular array of obstacles. Boundary-Layer Meteorol., 111, 363–415.

EFFECTS OF AIRBORNE PARTICLES ON CLOUDS AND PRECIPITATION

S. Solomos, G. Kallos, J. Kushta

University of Athens, School of Physics, University of Athens Campus, Bldg. Phys-5, 15784, Athens, Greece

INTRODUCTION

The amount of airborne particles that will nucleate and form cloud droplets depends on their number concentration, size distribution and chemical composition and also on atmospheric conditions. Dust particles are efficient ice nuclei (IN) and contribute to the formation of ice condensates in high clouds (DeMott et al., 2003a; Teller and Levin 2006). Also they interact with sea salt or anthropogenic pollutants, mainly sulfates and nitrates, thus forming particles that consist of a core of mineral dust with coatings of soluble material (Levin et al., 1996). The soluble coating on the dust particles converts them into efficient CCN while maintaining their ability as IN (Levin et al., 2005; Astitha and Kallos, 2008 ; Astitha et al., 2010). Sea- salt particles are also very efficient CCN (Gong at al., 2003). Most studies decouple aerosol properties from cloud and atmospheric dynamics and thus cannot account for all the feedbacks involved in aerosol-cloud-climate interactions. The effects of atmospheric composition on clouds and precipitation are not monotonic and may differ from one area to another. The complexity of the above processes and the possible interactions and feedbacks across all scales in the climate system, indicate the need for an integrated approach in order to examine the impacts of air quality on meteorology and vice versa (Stevens and Feingold, 2009). An integrated modeling approach has been used to describe such processes for idealized cases as well as for real case studies. The results presented here are from Solomos et al., 2010a and Solomos et al., 2010b where one can find more detailed description on these experiments. The interaction between dust and salt particles and their ability to act as CCN during a case study over the Eastern Mediterranean resulted in more vigorous convection and more intense updrafts. The clouds that were formed reached higher tops and accumulated precipitation was found to be closely related to aerosol properties. These results indicate the large portion of uncertainty that remains unresolved and the need for more accurate description of aerosol feedbacks in atmospheric models and climate change predictions.

MODELING SYSTEM

The Regional Atmospheric Modeling System (RAMSv6) (Pielke et al., 1992; Cotton et al. 2003) was the basis for developing the Integrated Community Limited Area Modeling System (ICLAMS)

(Solomos et al., 2010) used in this study. This new version of the model has been designed for air pollution and climate research applications and includes several new capabilities related to physical and chemical processes in the atmosphere. New developments include an interactive desert-dust and sea-salt module, biogenic and anthropogenic pollutants parameterization, gas/cloud/aerosol chemistry, explicit cloud droplet nucleation scheme and an improved radiative transfer scheme. The two-way interactive nesting capabilities of the model allow the use of regional scale domains together with several high resolution nested domains. This feature allows the simultaneous description of long range transport phenomena and aerosol-cloud interactions at cloud resolving scales.

CLOUD PROCESSES IN PRISTINE AND HAZY ENVIRONMENT

In order to examine some of the links and feedbacks between aerosol and cloud properties, we performed a set of “idealized” simulations for a convective cloud system over flat terrain. An unstable thermodynamic profile was used to initialize the model and explicit cloud droplet nucleation parameterization was invoked in every time step and grid point. The number of activated droplets was calculated from grid-cell aerosol, P, T, and updraft velocity. All tests were performed with exactly the same configuration except for the aerosol properties. Each run started at 12:00 UTC and lasted for six hours.

Table 1. Model characteristics for nine aerosol scenarios.

Aerosol Cases	Aerosol-cloud interaction	Aerosol-radiation interaction
Case1 (control run)	NO	NO
Case2 (only radiation interaction)	NO	YES
Case3 (constant aerosol – "pristine")	YES	NO
Case4 (constant aerosol – "hazy")	YES	NO
Case5 (prognostic aerosol - 1% hygroscopic dust)	YES	YES
Case6 (prognostic aerosol - 5% hygroscopic dust)	YES	YES
Case7 (prognostic aerosol - 10% hygroscopic dust)	YES	YES
Case8 (prognostic aerosol - 30% hygroscopic dust)	YES	YES
Case9 (prognostic aerosol - 5% hygroscopic dust + INx10)	YES	YES

Two scenarios were considered for the initial distribution of aerosol concentration, namely the "pristine" and the "hazy" scenario. The "pristine" scenario is representative of a remote area with a relatively clean atmosphere of total particle concentration 100 cm^{-3}, while the "hazy" scenario assumes a total concentration of 1500 cm^{-3}. Such high aerosol concentrations can be found near urban areas or industrial zones and are also typical during intense dust episodes. Further development of the cloud system and the final amount of precipitation depend on the cloud microphysical structure and on the interplay with ambient dynamics.

The cloud structure was very different between the two simulations. This is clearly shown in Figure 1. Two separate cloud systems were still distinct after 170 minutes of simulation for the "pristine" case while during the "hazy" case the two clouds had merged to one cell and an anvil was formed at the upper cloud layers. Also, the microphysical cloud properties varied significantly between the "pristine" and "hazy" scenarios.

In the "pristine" simulation, the cloud droplets number concentration remained low throughout the simulation. Fewer CCN had to compete for the same amount of water. So, large cloud and rain droplets were allowed to develop and the collection efficiency was enhanced. This allowed for increased autoconversion rates of cloud to rain droplets and early initiation of warm rain process. Intense precipitation started 100 minutes into the simulation, with precipitation rates reaching as high as 15 mm h^{-1} (Figure 2a).
In contrast, during the "hazy" aerosol environment, precipitation was suppressed at the early cloud stages. The number of cloud droplets for the "hazy" scenario was very high. As a result, the conversion rates of cloud droplets to rain droplets remained low and precipitation was inhibited (Figure 2a). Maximum precipitation rate

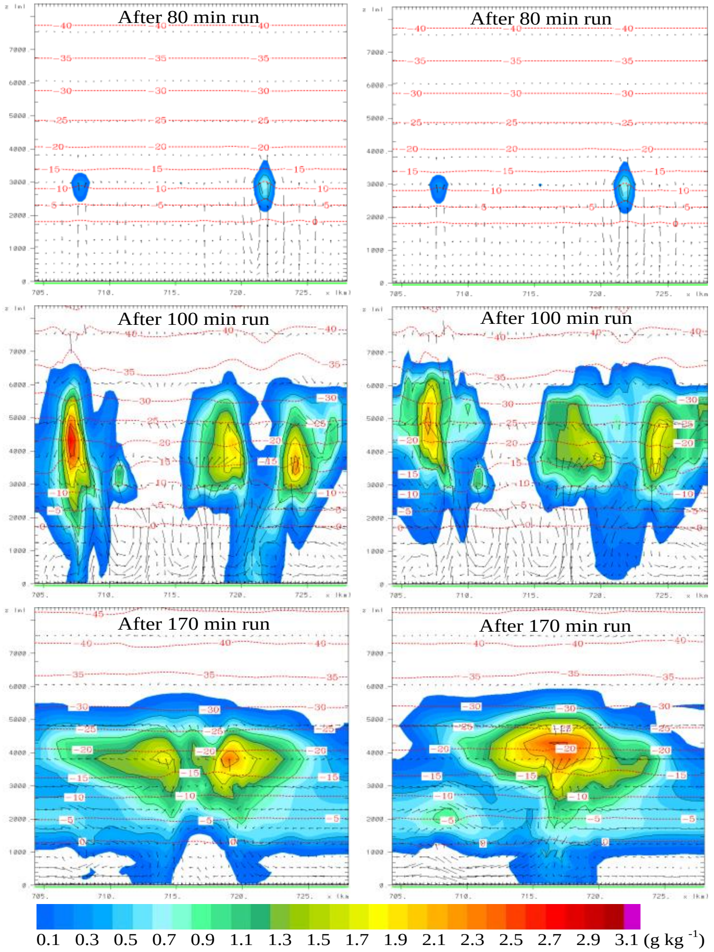

Figure 1. Total condensates mixing ratio (g kg^{-1}) for the "pristine" (left column) and the "hazy" (right column) scenarios.

at this stage was only 4 mm h^{-1} which is about 4 times less than the "pristine" scenario. However, the ice particles were almost double that of the "pristine" cloud and rain droplets coming from the melting of ice condensates produced a significant amount of rain between 150 and 210 minutes model time as seen also in Figure 2a. The accumulated precipitation over the entire domain was 286 mm for the "pristine" and 215 mm for the "hazy" case. Most of this difference can be attributed to the inhibition of precipitation during the early stages of cloud development in the "hazy" scenario.

EFFECTS OF GCCN ON CLOUDS AND PRECIPITATION

The impact of giant cloud condensation nuclei (GCCN) is also important for cloud processes and precipitation. When aerosol sizes are comparable to cloud droplet size - which is often the case for dust and sea-salt, kinetic limitations are imposed on cloud nucleation processes (Barahona et al., 2010). In order to examine the impact of GCCN on precipitation, we added a third coarser mode to the aerosol distribution with a median diameter of 10μm and a total concentration of 5 cm^{-3}. Adding GCCN to a hazy environment limited the number of cloud droplets that nucleated and as seen in Figure 2b the rainfall during the early stages of cloud development was increased. On the other hand, GCCN did not change significantly the warm stage precipitation for the pristine environment (Figure 2c). Precipitation rate was mainly affected by the number of activated cloud droplets. During the "pristine" case the clouds contained limited number of droplets which allowed them to grow fast to rain droplets. Adding a few GCCN for this case did not significantly change the cloud droplet spectrum in the model and so rainfall was not affected.

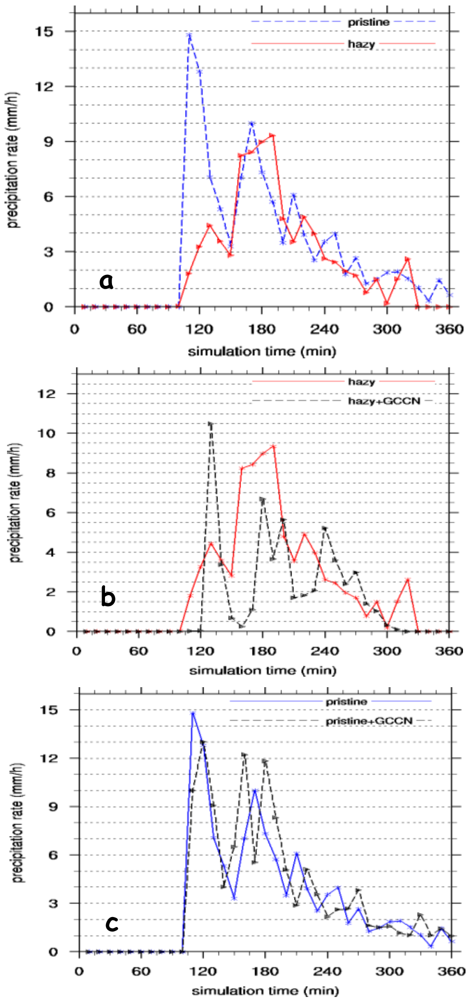

Figure 2. Maximum precipitation rate (mm h^{-1}) for: a) the "pristine" and "hazy" aerosol scenarios. b) the "hazy" and "hazy+GCCN" aerosol scenarios. c) the "pristine" and "pristine+GCCN" aerosol scenarios.

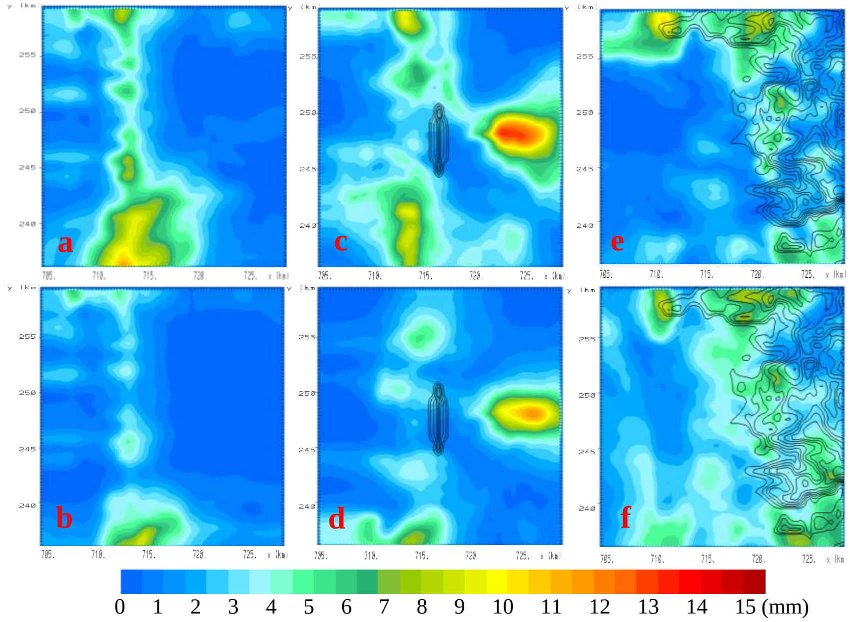

Figure 3. Four hour accumulated precipitation (colour palette in mm) and 50m topographic line contours. 1st row (a,c,e): "pristine" aerosol. 2nd row (b,d,f): "hazy" aerosol. 1st column: No topography (flat terrain). 2nd column: artificial obstacle vertical to the general flow. 3rd column: complex topography. The domain total precipitation for each case is: a) 12.28 m, b) 7.21 m, c) 16.77 m d) 11.01 m, e) 12.97, f)17.86.

EFFECTS OF TOPOGRAPHY ON PRECIPITATION

The simplistic approach to the interactions between airborne particles and clouds that is described in the previous sections is not always representative of real atmospheric conditions. For example, by adding topographic effects in a 3-D model configuration that is equivalent to the 2-D "pristine" and "hazy" model simulations resulted in substantially different spatial distribution of precipitation as shown in Figure 3. The impact of topography on precipitation was investigated for three cases, namely "flat terrain", "idealized hill" and "complex hilly area". The first case (flat terrain) considers no topographic features. In this case, atmospheric stability and cloud microphysics are the governing factors for the evolution of the cloud system. As seen in Figures 3 a, b, most of the precipitation was distributed over the western side of the domain for both "pristine" and "hazy" clouds but with different maxima ("pristine" case gave more precipitation). For the second run ("the idealized hill") the landscape remains the same as in the previous case but a 290 m high ridge with a N-S uniform orientation is added at the center of the domain. The combination of microphysics and cloud dynamics due to mechanical elevation over the hill resulted in a substantially different precipitation pattern that is shown in Figures 3 c, d. The distribution of precipitation for this case is clearly related to the location of the hill with more rain falling over the downwind area at the eastern part of the domain. Finally, the third case includes also the same landscape but the topography is representative of a complex hilly area with heights up to 700m. As illustrated in Figures 3 e, f, these topographic features resulted in a completely different distribution of precipitation. Such results indicate that the synergetic effects between the microphysical and macrophysical parameters that contribute in cloud and precipitation processes should be taken into account in relevant modeling studies on a combined way. Otherwise, the results may be misleading when compared to real atmospheric conditions.

EFFECTS OF DUST AND SALT PARTICLES ON CLOUD DEVELOPMENT

We focus on a case study that combines a low pressure system and a dust storm over the eastern Mediterranean. On 28 January 2003, the centre of the low moved from Crete through Cyprus accompanied by a cold front. Also, prevailing southwesterly winds over Northeastern Africa transported dust particles towards the coast of Israel and Lebanon. As illustrated in Figure 4, deep convective clouds were developed along the frontal line. The aerosol particles within the lowest two kilometers of the atmosphere were a mixture of dust and sea-salt. The number concentration of modelled dust and sea salt particles was tested against in-situ aircraft observations that were performed (between 7:30 and 9:30 UTC) at various heights inside the dust-storm area. The concentrations of modelled particles inside the dust layer were in satisfactory agreement with airborne measurements as illustrated in Figure 5, with a correlation coefficient R=0.89. These results indicate that the model is able to quantitatively reproduce the horizontal and vertical structure of the dust storm. The coexistence of salt and dust particles at heights below cloud base provided significant amounts of highly hygroscopic mixed particles.

Three different scenarios related to the properties of the aerosol particles during the model runs are discussed here. All model parameters were held constant except the percentage of dust particles containing soluble material, thus becoming effective CCN. In experiment 1 (EXP1), 5% of dust particles were hygroscopic while for experiment 2 (EXP2), this percentage was increased to 20%. EXP3 incorporated 5% hygroscopic dust while the concentration of IN in the model was multiplied by a factor of ten in the presence of

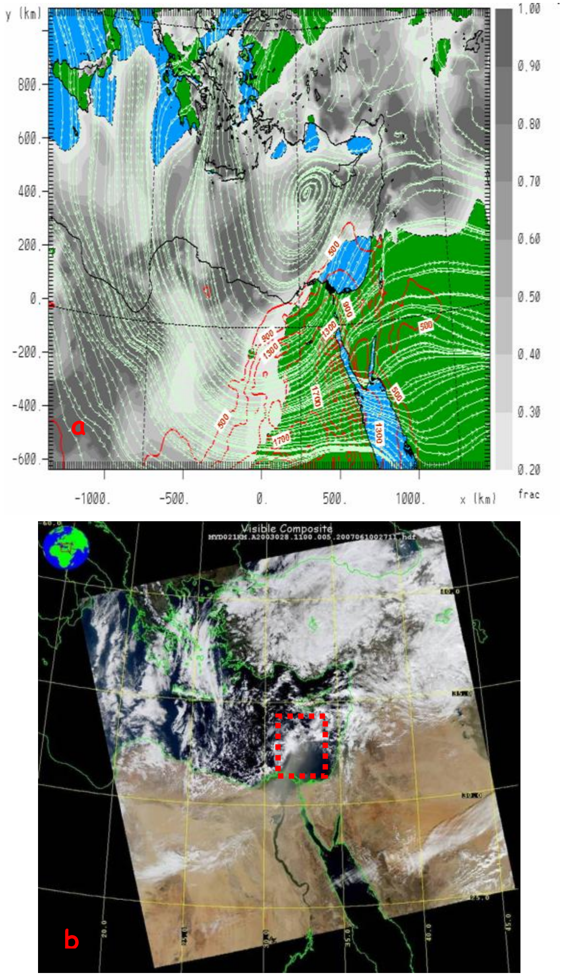

Figure 4. a) Cloud cover percentage (greyscale), streamlines at first model layer (green contours), dust - load (red contours in mg m^{-2}) and b) MODIS-Aqua visible channel, on 28 January 2003 1100, UTC. Dust transportation is obvious over the Southeastern part of Mediterranean. The red dashed rectangular indicates the location of convective clouds.

mineral dust. Increasing the percentage of hygroscopic dust particles from 5% to 20% increased also the concentration of small liquid droplets inside the cloud. This resulted in lower autoconversion rates of cloud to rain droplets and significant amount of water was transferred above freezing level. The EXP2 clouds reached higher tops, included more ice water content and the initiation of rainfall was in general delayed by almost 1 hour. In Figure 6, the cloud that was formed in the more pristine environment (EXP1) reached the maximum top at 9:00 UTC. The EXP2 cloud extended much higher (about 3km higher than EXP1), contained more ice, and eventually produced more rain (one hour later than EXP1; 10:00 UTC instead of 9:00 UTC). The EXP3 cloud also exhibited significant vertical development, with a structure and precipitation amounts similar to that of EXP2.

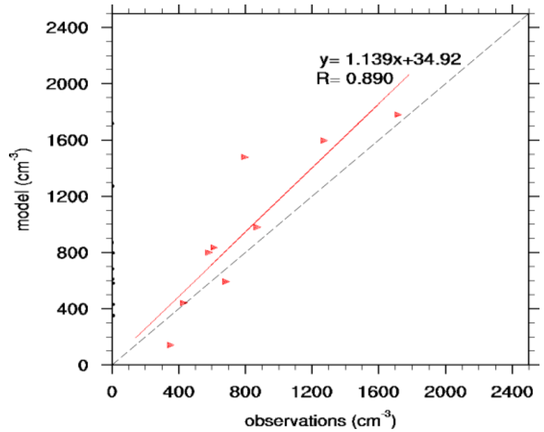

Figure 5. Comparison of aircraft measurements of natural particles with modeled dust and salt concentrations inside the dust layer (below 2km). The red line indicates the linear regression line while the dotted line indicates the y = x line.

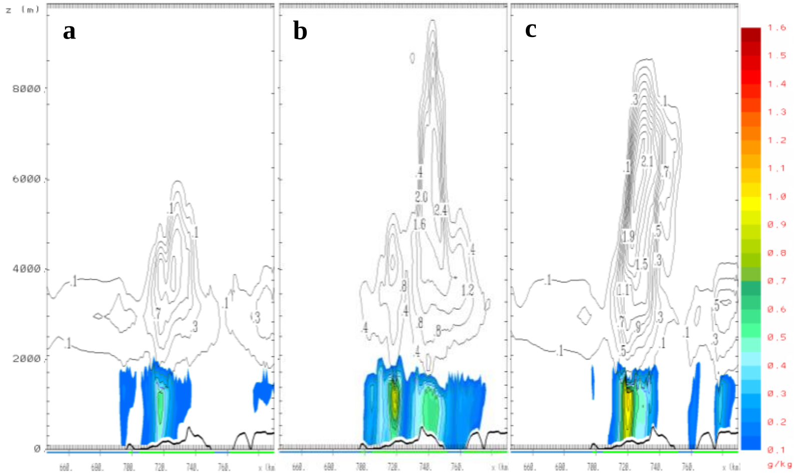

Figure 6. West to East cross-section of rain mixing ratio (color palette in g kg^{-1}) and ice mixing ratio (red line contours in g kg^{-1}) at the time of highest cloud top over Haifa. a) 9 UTC 29 January 2003 assuming 5% hygroscopic dust (EXP1). b) 10 UTC 29 January 2003 assuming 20% hygroscopic dust (EXP2). c) 9 UTC 29 January 2003 assuming 5% hygroscopic dust and INx10 (EXP3).

As illustrated in Figure 7a for the EXP2 case, significant amounts of liquid condensates existed in the middle and upper levels of the cloud and eventually froze in higher altitudes. The released latent heat invigorated convection and the equivalent potential temperature was increased (see Figure 7b with an arrow pointing to the area of increased equivalent potential temperature). After 10 minutes, strong updrafts reached up to 8 kilometers height and transferred condensates to the upper cloud layers as illustrated in Figure 7c. These condensates interact with the available IN in this area of the cloud for the formation of ice particles through

heterogeneous icing processes. These interactions between aerosols and cloud dynamics produce clouds with stronger updrafts that reach higher tops and finally produce heavier rainfall.

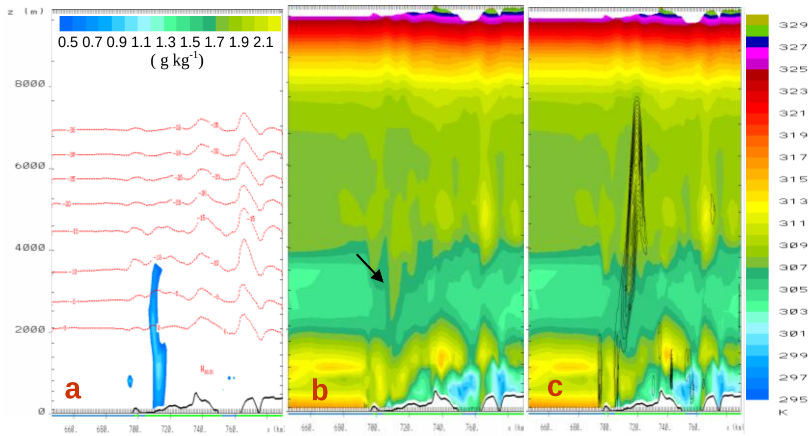

Figure 7. a) Liquid water mixing ratio (colour palette in g kg^{-1}) and ambient temperature (red contours in C^{O}) at 08:20 UTC. b) Equivalent potential temperature (colour palette in K) at 08:20 UTC. The arrow points at the area of increased Θ_e. c) Equivalent potential temperature (colour palette in K) and updrafts (black contours in m s^{-1}) at 08:30 UTC. The plots refer to EXP2.

EFFECTS OF DUST AND SALT PARTICLES ON PRECIPITATION

In order to examine the sensitivity of accumulated precipitation to aerosol properties, we performed a total of nine scenarios with the

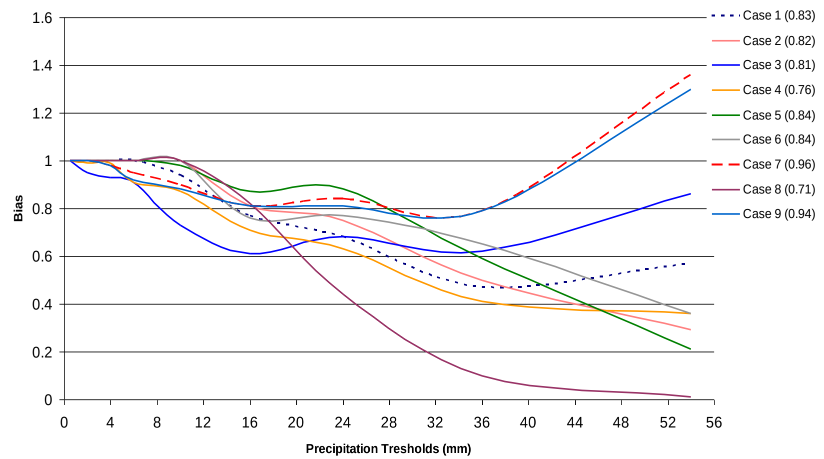

Number of available observations for each threshold: 0.5 (86), 2 (86), 4 (86), 6 (86), 10 (84), 16 (81), 24 (57), 36 (34), 54 (14)

Figure 8. Bias of the 24 hours accumulated precipitation for 86 stations and for nine scenarios of aerosol composition. The average bias for each scenario is specified in parenthesis after the legend labels. The number of available stations for each precipitation threshold is also denoted in parenthesis after the precipitation heights.

same model configuration but changing the chemical composition of airborne particles. The physio-chemical characteristics used on each run are shown in Table 1. The modelled 24-hour accumulated precipitation on 29 January 2003 for all nine cases was tested against ground measurements from 86 measuring stations over North Israel. Model bias scores were calculated for nine thresholds of accumulated precipitation, namely 0.5 mm, 2 mm, 4 mm, 6 mm, 10 mm, 16 mm, 24 mm, 36 mm and 54 mm. The results for each case and each precipitation threshold are shown in Figure 8. Biases equal to

one mean that the particular precipitation threshold was simulated as often as observed. Bias below unity indicates model underprediction and bias over one indicates overprediction.

Accumulated precipitation was found to be very sensitive to variations of the percentage of dust particles that can be activated as CCN and IN. Cases one to four exhibited more or less the same statistical performance that is probably explained from the use of constant prescribed aerosol properties for these runs. During the eighth case, the accumulated precipitation field was clearly underestimated due to the increased concentration of hygroscopic particles for this case. Increasing the number of CCN delayed the initiation of precipitation and resulted in the enhancement of ice concentrations. These ice crystals did not grow much because of the lack of water drops at higher levels. Most of these clouds evaporated before they managed to precipitate and the accumulated precipitation was underestimated.

CONCLUDING REMARKS

Several sensitivity tests with an integrated atmospheric model that includes online parameterization of aerosol processes, aerosol-radiation interaction, explicit cloud droplet activation scheme and a complete microphysics package indicated a significant response of cloud processes and precipitation to the variations of aerosol number concentration and also to the size distribution of the particles.

1. "Hazy" aerosol conditions suspended precipitation while the clouds that were formed in a "pristine" environment precipitated faster and produced more rain.

2. The distribution of accumulated precipitation was found to be much more sensitive to topographic variations than to aerosol number concentration and/or composition.
3. An increase of 15% in the concentration of soluble dust particles produced clouds that extended about three kilometres higher and the initiation of precipitation was delayed by almost one hour.
4. Variations between 1-30% in the amount of dust particles that were assumed to contain soluble material resulted in significant changes in cloud properties. The associated variations in the precipitation bias score were up to 80% for some thresholds.

These results illustrate the highly non-linear response of precipitation to aerosol properties. This study focuses mostly on investigating the mechanisms that are associated with the aerosol cloud interactions for a specific event. Therefore it is not possible to extract generic results. Nevertheless, this work represents one of the first limited area modelling studies for aerosol-cloud-radiation effects at the area of Eastern Mediterranean and could be used as a basis for future improvements and longer term studies. More intense combined modeling and observational surveys on the interactions between airborne particles and cloud processes at regional and local scale are necessary in order to improve our knowledge on the interactions between atmospheric chemistry and meteorology.

ACKNOWLEDGMENTS. This work has been supported by the European Union 6th Framework Program CIRCE IP, contract# 036961.

REFERENCES

Astitha, M. and Kallos, G.: Gas-phase and aerosol chemistry interactions in South Europe and the Mediterranean Region, Env. Fl. Mech.,doi:10.1007/s10652-008-91107.,2008.

Astitha, M., Kallos, G., Spyrou, C., O'Hirok, W., Lelieveld, J., and Denier van der Gon, H. A. C.: Chemically aged and mixed aerosols over the Central Atlantic Ocean – potential impacts, Atmos. Chem. Phys. 10, 5797-5822, 1020 doi:10.5194/acp-10-5797,2010.

Barahona, D., West, R. E. L., Stier, P., Romakkaniemi, S., Kokkola, H., and Nenes, A.: Comprehensively accounting for the effect of giant CCN in cloud activation parameterizations, Atmos. Chem. Phys., 10, 2467–2473, 2010.

Cotton W. R., Pielke, R. A. Sr., Walko, R. L., Liston, G. E., Tremback, C. J., Jiang, H. , McAnelly, R. L., Harrington, J. Y., Nicholls, M. E., Carrio, G. G. and J. P. Mc Fadden: RAMS 2001: Current status and future directions, Meteoro. and Atmos Phys 82, 5-29, 2003.

DeMott, P. J., Sassen, K., Poellet, M. R., Baumgardner, D., Rogers, D. C., Brooks, S. D., Prenni, A. J. and Kreidenweis, S. M.: African dust aerosols as atmospheric ice nuclei, Geophys. Res. Lett. 30 (14), 1732, doi:10.1029/2003GL017410, 2003a.

Gong, S. L.: A parameterization of sea-salt aerosol source function for sub- and super-micron particles, Global Biogeochemical Cycles 17 (4), p. 1097, 2003.

Levin, Z., Ganor, E. and Gladstein, V.: The effects of desert particles coated with sulfate on rain formation in the eastern Mediterranean, J. Appl. Meteorol., 35, 1511-1523, 1996.

Levin, Z., Teller, A., Ganor, E., and Yin, Y.: On the interactions of mineral dust, sea-salt particles and clouds: A measurement and modeling study from the Mediterranean Israeli Dust Experiment campaign, J. Geophys. Res., 110, D20202, doi: 10.1029/2005JD005810, 2005.

Pielke, R. A., Cotton, W. R., Walko, R. L., Tremback, C. J., Lyons, W. A., Grasso, L. D., Nicholls, M. E., Moran, M. D., Wesley, D. A., Lee, T. J. and Copeland, J. H.: A comprehensive meteorological modeling system—RAMS, Meteor. Atmos. Phys.,49, 69–91, 1992.

Solomos, S., Kushta, J., Kallos, G.: Effects of natural and anthropogenic particles on cloud formation and precipitation – A modeling study, 31st NATO/CCMS International Technical Meeting on Air Pollution Modeling and its Applications (ITM) , Turin, Italy, September, 2010a.

Solomos, S., Kallos, G., Kushta, J.,Astitha, M., Tremback, C., Nenes, A., Levin, Z.: An integrated modeling study on the effects of mineral dust and sea salt particles on clouds and precipitation, Atmos. Chem. Phys. Discuss., 10, 23959–24014, 2010, doi:10.5194/acpd-10- 23959-2010b

Stevens, B. and Feingold, G.: Untangling aerosol effects on clouds and precipitation in a buffered system, Nature, 461, doi:10.1038/nature08281, 2009.

Teller, A. and Levin, Z.: The effects of aerosols on precipitation and dimensions of subtropical clouds; a sensitivity study using a numerical cloud model, Atmos. Chem. And Phys. 6, 67–80, 2006

Future events

NATO ADVANCED RESEARCH WORKSHOP - CLIMATE CHANGE, HUMAN HEALTH AND NATIONAL SECURITY
Dubrovnik, Croatia, 28 - 30 April 2011

Participants of this workshop will explore the intricate relationships between climate change, human health and the security of nations, and how these relationships are mediated by conflicts arising from scarcity of water resources, impacts onfood production, rising energy demands, and deteriorating human health and behavioral

changes. The intended outcome is the publication of a document outlining the state-of-the-art of understanding of these issues and their interrelationships as well as identification of future research and policy and management needs.

Participation in this workshop is by invitation only with each attendee presenting an overview of the current understanding of their field followed by a discussion on how their work is related to the theme of the workshop.

For more information, please visit the website: http://www.nd.edu/~dynamics/NATOWorkshop.htm

INTERNATIONAL WORKSHOP "INTEGRATION OF GEOSPHERES IN EARTH SYSTEMS: MODERN QUERIES TO ENVIRONMENTAL *PHYSICS, MODELLING, MONITORING & EDUCATION*' 30.04-3.05.11, DUBROVNIK, CROATIA – JOINT MEETING OF THE FOUR ONGOING PROJECTS:

- MEGAPOLI "Megacities: Emissions, urban, regional and Global Atmospheric POLlution and climate effects, and Integrated tools for assessment and mitigation (FP7-ENV-2007.1.1.2.1 project 212520, 2008-2011, coordinator A.A. Baklanov) http://megapoli.info
- MEGAPOLIS "Integration technologies for evaluation of atmospheric pollution in megacities on regional and global scales based on air, space and ground monitoring for reduction of negative consequences of anthropogenic impacts" (Russian national project, 2009-2011, coordinator

V.G. Bondur) http://www.geogr.msu.ru/news/news_detail.php?ID=2288

- PBL-PMES "Atmospheric Planetary Boundary Layers (PBLs) - Physics, Modelling and Role in Earth Systems" (FP7 Specific Programme IDEAS, ERC Advanced Grant No. 227915, 2009-2013, coordinator S.S. Zilitinkevich) http://pbl-pmes.fmi.fi/
- QualiMet "Development of Qualification Framework in Meteorology" (EU TEMPUS project No. 159352, 2010-2013, coordinator S.S. Zilitinkevich) http://qualimet.net/

1st WORLD SCIENTIFIC CONFERENCE PETRA 2011 (POLLUTION AND ENVIRONMENT-TREATMENT OF AIR)
Prague, Czech Republic, 17 - 20 May, 2011

The Conference is held under the auspices of the Czech Ministry of the Environment and the Czech Ministry of Industry and Trade and it is devoted to the protection of global climate. The main objective of the Conference is to concentrate experts from all over the world to introduce the latest scientific and practical knowledge in the branch and to exchange their experience in an effort to find common ways to cooperate. The conference is intended for researchers and wider public concerned about the given issue.

More information at:
http://odour.webnode.cz/en/konference/konference-petra-2011/

11th INTERNATIONAL MULTIDISCIPLINARY SCIENTIFIC GEO-CONFERENCE & EXPO SGEM2011 - MODERN MANAGEMENT OF MINE PRODUCING, GEOLOGY AND ENVIRONMENTAL PROTECTION
Albena, Bulgaria, 19 - 25 JUNE, 2011

The SGEM GeoConference focuses on the latest findings and technologies in surveying geology and mining, ecology, and management, in order to contribute to the sustainable use of natural resources. In this regards all theoretical, methodological and conceptual reports presenting contemporary geoscience development and problems solving ideas are expecting with a great interest. Special attention will be given to reports, proposing science based ideas for decision-making and adaptation to the new reality of global changes. All accepted papers will be published in a conference proceedings indexed by ISI Web of Knowledge, Web of Science.

The conference is the best platform for knowledge and experience shearing in the field of geosciences. Special workshops will be held as a parallel to the SGEM2011 conference sessions. This is an additional opportunity for SGEM participants to exchange views and to learn about best practice in environmental and geo researches application and management.

T O P I C S:
1. Section „Geology"
2. Section „Hydrogeology, Engineering Geology and Geotechnics"
3. Section „Exploration and Mining"
4. Section „Mineral Processing"
5. Section „Oil and Gas Exploration"

6. Section „Applied and Environmental Geophysics"
7. Section „Geodesy and Mine Surveying"
8. Section „Photogrammetry and Remote Sensing"
9. Section „Cartography and GIS"
10. Section „Informatics"
11. Section „Geoinformatics"
12. Section „Micro and Nano Technologies"
13. Section „Hydrology and Water Resources"
14. Section „Marine and Ocean Ecosystems"
15. Section „Forest Ecosystems"
16. Section „Soils"
17. Section „Air Pollution and Climate Change"
18. Section „Renewable Energy Sources and Clean Technologies"
19. Section „Nuclear Technologies"
20. Section „Ecology and Environmental Protection"
21. Section „Recycling"
22. Section „Environmental Economics"
23. Section „Education and Accreditation"
24. Section „Environmental Legislation, Multilateral Relations and

For more information, please visit the website: www.sgem.org

14TH CONFERENCE ON THE ACCENT-PLUS SYMPOSIUM "AIR QUALITY AND CLIMATE CHANGE: INTERACTIONS AND FEEDBACKS", Urbino, Italy, 13 - 16 September 2011

More information at:
http://www.uniurb.it/SA/AccentPlus2011/leaflet2011.html and
http://www.uniurb.it/SA/AccentPlus2011/information2011-date.html

2ND WORKSHOP "INFORMATICS & INTELLIGENT SYSTEMS APPLICATIONS FOR QUALITY OF LIFE INFORMATION SERVICES" ISQLIS - ORGANIZED IN THE FRAME OF THE 12TH EANN (ENGINEERING APPLICATIONS OF NEURAL NETWORKS) AND OF THE 7TH AIAI (ARTIFICIAL INTELLIGENCE APPLICATIONS AND INNOVATIONS) CONFERENCES, CORFU, GREECE, 15 – 18 SEPTEMBER 2011

Paper submission deadline: 30 April 2011
More information at:
http://delab.csd.auth.gr/eann2011/isqlis.html

14TH CONFERENCE ON HARMONISATION WITHIN ATMOSPHERIC DISPERSION MODELLING FOR REGULATORY PURPOSES, KOS, GREECE, 2 – 6 OCTOBER 2011

More information at: http://www.harmo14.gr/

THE SIXTH INTERNATIONAL SYMPOSIUM ON NON-CO_2 GREENHOUSE GASES (NCGG-6), SCIENCE, POLICY AND INTEGRATION, AMSTERDAM, THE NETHERLANDS, 2 – 4 NOVEMBER 2011

More information at: http://www.eurasap.org/FutureEvents.html

News

ON THE UK ATMOSPHERIC DISPERSION MODELLING LIAISON COMMITTEE (ADMLC)

The Atmospheric Dispersion Modelling Liaison Committee (ADMLC) was formed in 1995. Although ADMLC was formed to consider primarily the nuclear industry it has expanded its range of interests and its membership to more fully reflect the needs of industrial and regulatory organisations. Its main aim is to review current understanding of atmospheric dispersion and related phenomena for application primarily in authorization or licensing of discharges to atmosphere resulting from industrial, commercial or institutional sites. The Committee's emphasis is on fixed sources,

rather than transport sources, and covers both routine releases and releases in accident or "upset" conditions.

ADMLC facilitates the exchange of ideas and highlights where there are gaps in knowledge. It tries to provide guidance to, and to endorse good practice in, the dispersion modelling community. It is keen to promote relationships with other dispersion modelling groups. The Committee has hosted workshops, and welcomes ideas for joint meetings with other organisations or for workshops on particular topics.

Organisations on the ADMLC

- AMEC
- Atomic Weapons Establishment, Aldermaston
- Defence Science and Technology Laboratory
- Department for Energy and Climate Change (DECC)
- Department for Environment Food and Rural Affairs (Defra)
- Environment Agency
- Food Standards Agency
- Health and Safety Executive
  Methodology and Standards Development Unit, Hazardous Installations Directorate
  Nuclear Installations Inspectorate
  http://www.hse.gov.uk/nsd/
- Health Protection Agency, http://www.hpa.org.uk/
- Home Office
- Met Office
- Nuclear Department, HMS Sultan
- Scottish Environment Protection Agency
- Shell Global Solutions
- Westlakes Research Institute

More information at: http://www.admlc.org.uk/index.htm

EUROPEAN ASSOCIATION FOR THE SCIENCE OF AIR POLLUTION MEMBERSHIP FORM 2011

Please fill out the details below and return to:
Carlos Borrego
IDAD - Instituto do Ambiente e Desenvolvimento
Campus Universitário
3810-193 Aveiro (PORTUGAL)
E-mail: eurasap@ua.pt

I renew my membership/ I apply for registration* as individual/corporate* member of EURASAP (* Delete whatever is not applicable).

(1) Family name...
(1) First name...
Title...
(1)Organisation..
....
(1) Address
....
....
....
(1)Tel...Fax...
(1) E-mail..
Internet...
(1) **Mandatory fields**

EURASAP subscription fees (please, circle what applies):

1. 40 EURO for individual members in Europe
2. 50 EURO for individual members outside Europe
3. 250 EURO for corporate members in Europe
4. 300 EURO for corporate members outside Europe
5. 15 EURO for students
6. No fee in case personal or social circumstances prevent you from paying the fee (after approval by Direction)
7. Extraordinary fee (higher than those above, after approval by Direction)
Note: The payment is only possible in **Euro**.

Payment can be done by credit card (VISA or MasterCard only) or bank transfer. The membership forms signed for credit card payment should be mailed to Carlos Borrego to the address given above. Please, mail also the membership form in case of bank transfer. **Cross your options below**. Thank you.

☐ I need the invoice* receipt* (* Delete whatever is not applicable). in personal name* institution above* (* Delete whatever is not applicable).

☐ Bank transfer
Name: BES - Banco Espírito Santo
Address: Avenida Dr. Lourenço Peixinho, 5 - 3800 Aveiro (Portugal)
IBAN: **PT50 0007 0230 00314300001 11** BIC/ Swift: **BESCPTPL**

☐ Credit card payment
Credit card type .... Credit card number....................................
Expiry date .... CVV2 (3 digits of the back of your card)................
Amount of money to pay.........................
Date.. Signed..

This form is mailed to you only once per year!
It is available to download it from http://www.eurasap.org